

N 70 18866

NASA CR 108130

TECHNICAL REPORT

INVESTIGATION OF WARM FOG PROPERTIES AND FOG MODIFICATION CONCEPTS

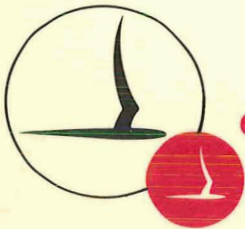
By: Warren C. Kocmond and William J. Eadie

CAL No. RM-1788-P-22

Prepared for:
Office of Aeronautical Research
National Aeronautics and Space Administration
Washington 25, D.C.

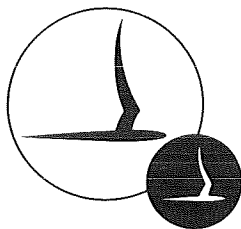
Fifth Annual Summary Report
Contract No. NASr - 156
December 31, 1969

**CASE FILE
COPY**



CORNELL AERONAUTICAL LABORATORY, INC.

OF CORNELL UNIVERSITY, BUFFALO, N. Y. 14221



CASE FILE
COPY

CORNELL AERONAUTICAL LABORATORY, INC.
BUFFALO, NEW YORK 14221

PROJECT FOG DROPS
INVESTIGATION OF WARM FOG PROPERTIES
AND FOG MODIFICATION CONCEPTS

FIFTH ANNUAL SUMMARY REPORT

CONTRACT NO. NASr-156

CAL REPORT NO. RM-1788-P-22

DECEMBER 31, 1969

PREPARED BY:

Warren C. Kocmond

Warren C. Kocmond

William J. Eadie

William J. Eadie

APPROVED BY:

Roland J. Pille'

Roland J. Pille', Assistant Head
Applied Physics Department

TABLE OF CONTENTS

<u>Section</u>	<u>Page</u>
LIST OF FIGURES	iii
LIST OF TABLES	v
ACKNOWLEDGMENTS	vi
ABSTRACT	vii
I. INTRODUCTION	1
II. DISSIPATION OF NATURAL FOG IN THE ATMOSPHERE	3
A. Instrumentation and Equipment	3
B. Fog Characteristics	5
C. Fog Seeding Results - Ground Seeding	10
D. Fog Seeding Results - Aerial Seeding	14
E. Conclusions from 1968 Field Experiments	18
III. COMPUTER MODELING	21
A. Description of the Basic Model	22
B. Modeling of the Effects of Turbulent Diffusion	27
C. Results	31
IV. LABORATORY EXPERIMENTS WITH SEEDING AGENTS OTHER THAN NaCl	47
A. Test Procedure	47
B. Summary of Results	49
C. Conclusions	59
REFERENCES	60
APPENDIX A	A-1

LIST OF FIGURES

<u>Figure No.</u>		<u>Page</u>
1	Mobile Seeding Apparatus	4
2	Vertical Profiles of Valley Fog Parameters (Average Data from Eight Fogs)	6
3	Drop Size Distributions at Four Levels in a Valley Fog - Elmira, N. Y. 30 August 1968	7
4	Saturated Specific Humidity as a Function of Temperature	9
5	Location of Seeding Unit and Transmissometers at Experimental Field Site - Chemung County Airport, Elmira, New York, September 8, 1968	12
6	Comparison of Drop Size Distributions for Natural and Seeded Fog, Sept. 8, 68.	14
7	Drop Size Distributions at Four Levels in a Valley Fog Prior to Seeding - Elmira, New York 16 October 1968	16
8	Three Photo Sequence of Fog Clearing	17
9	Comparison of Drop Size Distributions for Seeded and Unseeded Natural Fog, Elmira, 10/16/68	19
10	Fog Drop Distribution Used in Computer Simulation of Fog Seeding by Aircraft	33
11	Size Distribution of NaCl Seeding Material Used in Computer Simulation of Fog Seeding by Aircraft	34
12	Computed Curves of Visibility vs. Height as a Function of Seeding Rate and Time after Deposition of NaCl Seeding Material at Top of Fog	35
13	Computed Curves of Vertical Visibility vs. Time as a Function of Seeding Rate for Aerial Seeding with 20 μ Diameter NaCl Particles under Near-Neutral Stability and a One Knot Wind	38
14	Computed Curves of Vertical Visibility vs. Time as a Function of Particle Diameter for Aerial Seeding with 500 lbs of NaCl per Nautical Mile under Near-Neutral Stability and a One Knot Wind	42
15	Computed Curves of Vertical Visibility vs. Time as a Function of Seeding Rate for Aerial Seeding with a 15 to 40 μ Diameter Size Distribution of NaCl Particles under Near-Neutral Stability and a One Knot Wind	43

LIST OF FIGURES (Cont'd.)

<u>Figure No.</u>		<u>Page</u>
16	Computed Curves of Vertical Visibility vs. Time as a Function of Seeding Rate for Aerial Seeding with 20 μ Diameter NaCl Particles under Near-Neutral Stability and a Five Knot Wind	45
17	The 600m ³ Test Chamber at Ashford, New York	48
18	Visibility as a Function of Time for a Seeded and Control Fog	52
19	Drop Size Distribution for a Control Fog and a Seeded Fog at T = 20 min. Na ₂ HPO ₄	53
20	Visibility as a Function of Time for a Seeded and Control Fog	57
21	Drop Size Distribution for a Control Fog and a Seeded Fog at T = 25 min. Polyelectrolyte 'B'	58

LIST OF TABLES

<u>Table No.</u>		<u>Page</u>
I	Comparison of Fog Characteristics	5
II	Visibility Improvement Factors for Some Seeding Agents Tested in the 600m ³ Cloud Chamber	50
III	Effects of Particle Size Distribution for NaCl Seedings in the 600m ³ Cloud Chamber (5.0gm Payloads).	54
IV	Polyelectrolyte Seeding Experiments	55

ACKNOWLEDGMENTS

The authors are indebted to Mr. Roland J. Pilić for his many contributions throughout the program, especially during the design and planning of the field experiments, and for his assistance in preparing this text.

Special thanks are given to Mr. Eugene Mack for his valued assistance in the collection and analysis of data; to Mr. George Zigrossi who has been responsible for maintaining and improving much of the instrumentation used in this study; and to Mr. Calvin Easterbrook who designed the transmissometers used for measuring visibility in fog.

Thanks are also due the many members of the Atmospheric Physics and Dynamic Meteorology Sections who unselfishly gave of their time to participate in the field experiments.

Finally, we express our gratitude to Mr. Glenn Banfield, Airport Manager of the Chemung County Airport, Elmira, New York, for his cooperation and assistance during the field portion of the program and for his permission to utilize airport facilities during our fog seeding experiments.

ABSTRACT

Field experiments were performed to determine the effects of seeding natural valley fog with carefully sized hygroscopic materials. Both ground-based and aerial seeding experiments were conducted. Airborne seedings were found to be most effective in causing fog dissipation. In one experiment, 700 lbs of carefully sized NaCl particles were disseminated onto the fog top from a light aircraft. Visibility in the seeded area increased from 300 feet to 2600 feet within fifteen minutes after seeding. Fifteen minutes later the opening was closed by fog diffusing into the seeded region from the sides.

Analysis of data has shown that the initial improvement in visibility resulted from a favorable shift in the fog drop-size distribution. Subsequent improvements were due to a decrease in the liquid water content of the fog as a result of precipitation of the large droplets formed on the seeding nuclei.

A computer model has been developed to simulate warm fog seeding experiments. The effects of several variables on fog modification have been studied. The influence of particle size distribution, seeding rate, and horizontal diffusion have been investigated with the model and are discussed in the text.

Laboratory tests of various hygroscopic seeding agents were performed in a 600 m³ cloud chamber. The results, which are summarized in this report, have shown that NaCl, urea, certain phosphates and a 9:1 solution of ammonium nitrate • urea • water are effective in promoting fog dissipation. Results of laboratory tests with sized polyelectrolytes suggest that these materials are ineffective as seeding agents.

I. INTRODUCTION

Occurrences of dense fog in the United States frequently result in costly delays and cancellations to airlines and often pose a serious hazard to pilots attempting landings under marginal visibility conditions. Recognizing a need for further research in the area of warm fog modification NASA authorized Cornell Aeronautical Laboratory in 1963 to begin an investigation of warm fog properties and fog modification principles. Since that time the objective of Project Fog Drops has been to obtain a firm understanding of the physical and dynamic properties of fog with the expectation that this approach might lead to the development of a practical concept for improving visibility in naturally occurring fog.

Initially, attention was given to developing physical and dynamic fog models and to conducting experiments to determine more about the diffusional growth rates of fog droplets in a supersaturated environment. Instrumentation was developed for observing the concentrations of nuclei in the atmosphere that are responsible for cloud and fog formation. Techniques for enhancing or retarding droplet growth and evaporation rates were studied and experiments were performed to determine if the coalescence behavior of fog droplets could be significantly altered. Later, during the program's third year, laboratory tests of suggested concepts for fog suppression were performed. Additional measurements of the microphysical characteristics of fog were obtained, and daily observations of cloud nuclei were continued and cataloged for comparison with our earlier observations.

As a result of these studies, a concept evolved for improving visibility in fog by seeding with hygroscopic nuclei of carefully controlled size. After considerable theoretical development, a series of laboratory tests were performed to determine if the concept could be applied on a larger scale, i. e., to natural fog. A computer model was simultaneously developed to complement the laboratory studies and to provide a basis for designing field experiments which would follow. The model, which is designed to test the consequences of seeding fogs with hygroscopic materials, provided additional insight into the problems of fog modification and helped shape much of our subsequent thinking.

Field tests of the concept were performed during the summer of 1968. Data accumulated during these tests were analyzed during the months that followed and are presented in this report. Results of our computer modeling effort are also described in detail. A concurrent study involving laboratory tests of a variety of hygroscopic seeding agents is reported on in this summary report. For brevity, results of previous years' investigations will not be discussed here; rather, the interested reader is encouraged to review the detailed discussions that are presented in NASA Contractor Reports CR-72, CR-368, CR-675, CR-1071, and SP-212.

II. DISSIPATION OF NATURAL FOG IN THE ATMOSPHERE

During the late summer and early fall months of 1968, fog seeding experiments were conducted at the Chemung County Airport near Elmira, New York. The primary objective of these experiments was to determine the effects of seeding dense natural fog with carefully sized hygroscopic particles. Our intent was to evaluate the concept by seeding fogs from the ground, and if necessary, perform aerial seeding experiments during the latter part of the fog season. A total of 25 experiments were conducted with ground seeding apparatus during the period May-September 1968. Six aerial seedings of dense valley fog were performed during a three week period in October 1968. Data collected during several of these experiments have now been analyzed and the results are presented here.

After reviewing the climatology of several locations, the vicinity of Elmira, New York was selected for fog seeding experiments because of its high fog frequency and relative proximity to the Laboratory. On the average, about 30 dense fogs formed in the Chemung Valley near Elmira between the months of May and October. Most of the fogs appeared to be of the radiation type, forming during cloudless nights between the hours of 12 midnight and 6 a.m. The presence of a nearby airfield on one of the adjacent ridges made this site a particularly appealing one for airborne seeding trials.

A. Instrumentation and Equipment

Initially, fogs were seeded from the ground using the mobile seeding apparatus pictured in Figure 1.

During operation, hygroscopic nuclei of controlled sizes were fed from within the camper to a nitrogen-driven particle disseminator. The nuclei were then transferred by means of a high-velocity nitrogen stream through copper ducting to a region near the center of, and slightly above, a 9-ft diameter, three-bladed propeller. Here, the particles were injected into the airstream and lifted to altitudes varying from a few feet to several hundred feet depending on the prop speed and atmospheric stability. A

protective steel shroud, which also enhanced air flow around the prop, was positioned around the propeller hub assembly. Dry nitrogen, used for transferring nuclei to the prop wash, was stored in large high pressure cylinders mounted on the sides of the rig.



Figure 1 MOBILE SEEDING APPARATUS

Instrumentation for making observations in fog included:

1. A Piper Aztec airplane equipped to measure drop sizes and temperatures at various altitudes in fogs and to provide photo reconnaissance of the seeded area. Photographic equipment consisted of two 70 mm Hasselblad cameras mounted in the fuselage of the aircraft.
2. A mobile van carrying instrumentation for measuring drop sizes, liquid water content, visibility, nucleus concentration and temperature in seeded and unseeded fog.
3. Four transmissometers for measuring visibility at selected locations on the airport grounds.

4. A CAL vehicle for locating the path of the seeding material.

B. Fog Characteristics

Prior to seeding experiments, the CAL Piper Aztec was sent aloft through the dense fog to gather data on drop sizes, vertical temperature distribution and fog depth. Supplementary data, which included measurements of visibility, liquid water content, drop sizes, and nucleus concentration were obtained at the ground. In Table I typical physical characteristics of the valley fogs in Elmira, New York are compared with the radiation and advection fog models developed during the first year of this program (Jiusto, 1964). The data for the Elmira fogs represent averages of measurements made four feet above the surface in 13 fogs.

TABLE I
COMPARISON OF FOG CHARACTERISTICS

<u>Fog Parameter</u>	<u>Radiation Fog</u>	<u>Advection Fog</u>	<u>Valley Fog - Elmira, NY</u>
Average drop diameter	10 μ	20 μ	18 μ
Typical drop diameter range	4-36 μ	6-64 μ	4-50 μ
Liquid water content	110 mg m ⁻³	170 mg m ⁻³	160 mg m ⁻³
Droplet concentration	200 cm ⁻³	40 cm ⁻³	55 cm ⁻³
Visibility	100 m	300 m	100 m
Vertical depth	100-300 m	200-600 m	100-200 m

As shown, the data for the valley fogs and the advection fogs are similar. In Figure 2 vertical profiles of several pertinent fog parameters are shown for average data obtained in eight Elmira valley fogs. The data were obtained during take-off and ascent of the CAL Piper Aztec in the fogs. Values of drop concentration and liquid water content were computed from measured drop distributions assuming a constant visibility as a function altitude. (It is recognized that visibility is not constant; however, the results of computations are intended to provide an indication of trends in the data rather

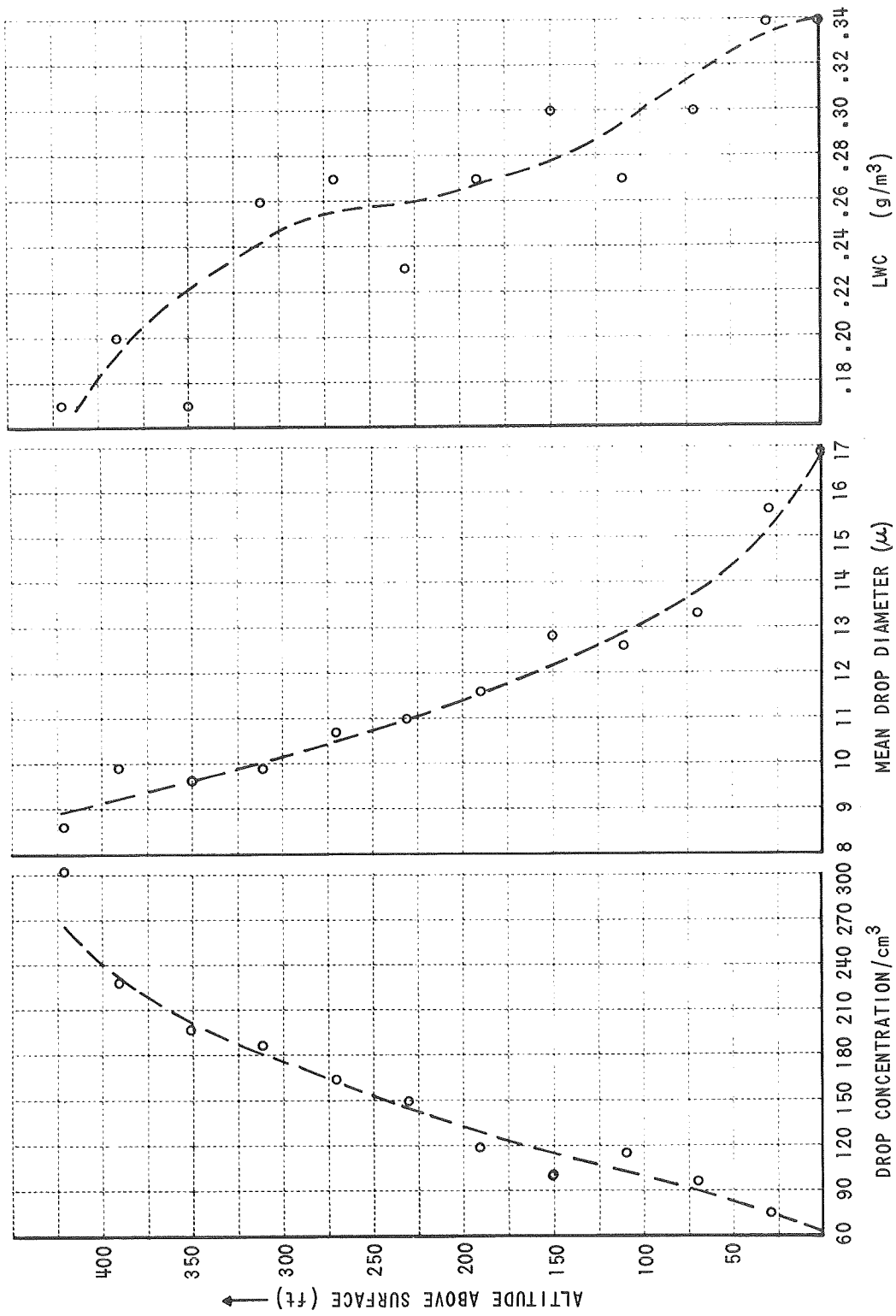


Figure 2 VERTICAL PROFILES OF VALLEY FOG PARAMETERS
(AVERAGE DATA FROM EIGHT FOGS)

than absolute measures.) Note the steady decrease in average drop diameter as a function of height above fog base. Accompanying the decrease in drop size is an increase in drop concentration, suggesting that conditions typical of radiation fog (i.e., high concentration of small drops) exist only in the upper portion of the fog. Similarly the liquid water content in the valley fog decreases steadily from a high value near the fog base to somewhat lower values near the top.

In Figure 3, selected drop size distributions are shown for four levels within a representative fog. Also shown for each distribution are the average drop diameter and computed values of drop concentration and liquid water content. Again the rather pronounced shift in drop sizes toward smaller values near the fog top is apparent.

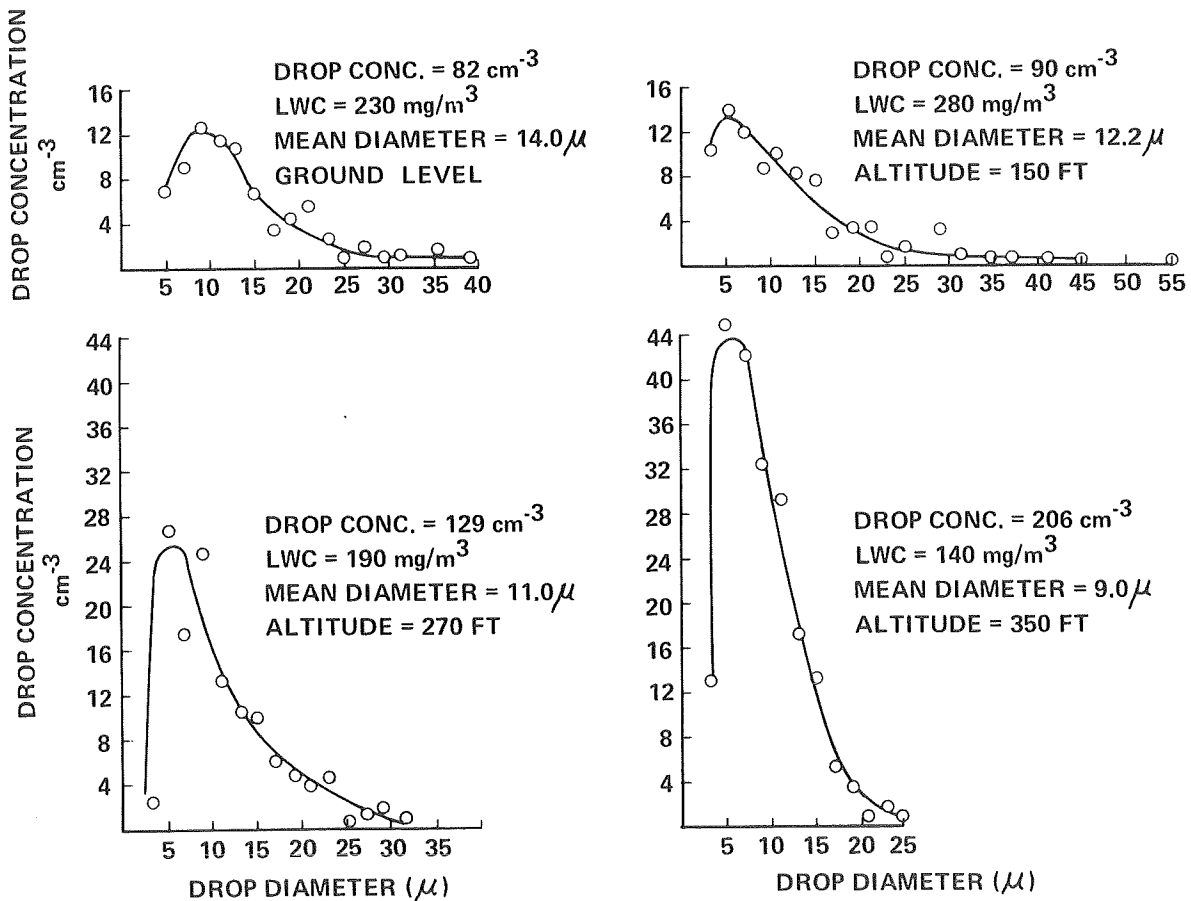


Figure 3 DROP SIZE DISTRIBUTIONS AT FOUR LEVELS IN A VALLEY FOG - ELMIRA, N.Y. 30 AUGUST 1968

Repeated observations of the formation of fog at the field site suggested that mixing of the nearly saturated layers of air in the valley govern the fog formation process and, as well, shape the drop size distribution and liquid water content of the fog. As always, a variety of other mechanisms involving energy, moisture and heat exchange are also important factors in fog development.

We have noticed that during the early evening, moderate breezes frequently blow across the valley and prevent significant fog formation. As the ambient winds subside, drainage from the hills begins to predominate and surface winds in the valley become aligned with the orientation of the valley. Radiational cooling of the earth's surface and subsequent loss of heat from the lowest layers of air to the ground produce nearly saturated conditions close to the surface. Temperature profiles obtained shortly before fog formation at Elmira have shown that substantial inversions, frequently exceeding 3°C in 100 m, exist in the lowest few hundred feet of air. Once cold air drainage predominates, saturated surface air from the hillside tends to displace the somewhat warmer, nearly saturated air in the valley and, in the process, mixing occurs.

In the phase diagram (Figure 4) conditions typical of the valley atmosphere prior to fog formation are illustrated. If, as shown, two parcels of moist air, A and B, having different temperatures and relative humidities are mixed, significant supersaturation will occur and fog will form. The characteristics of the mixture of the two air masses will be represented by some point on the straight line connecting A and B.

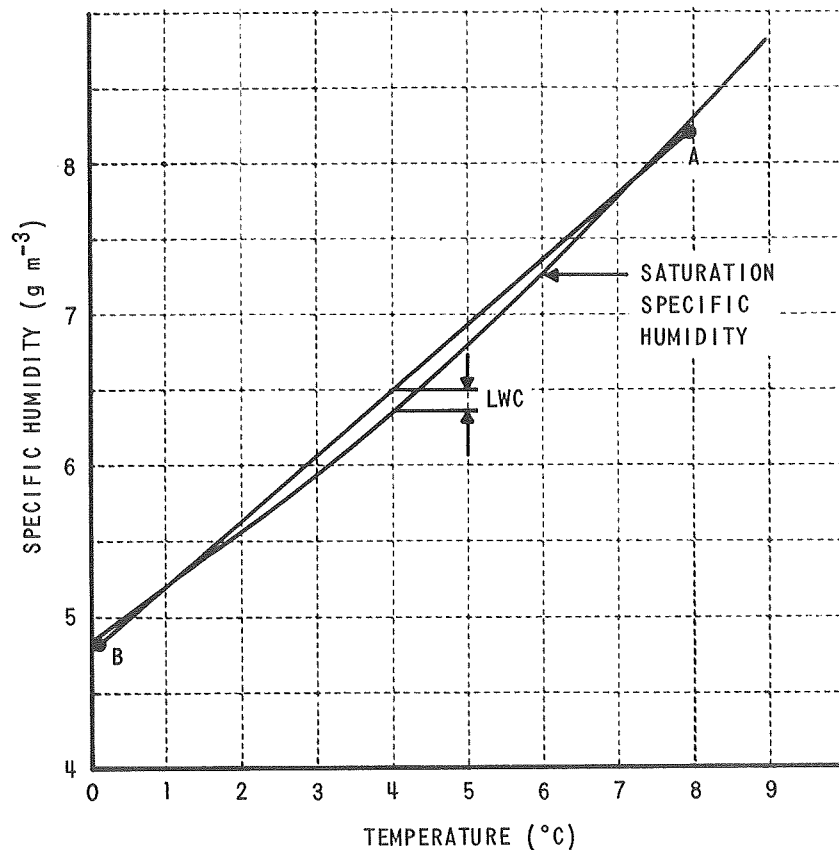


Figure 4 SATURATED SPECIFIC HUMIDITY AS A FUNCTION OF TEMPERATURE

In the formation of valley fog, initial mixing occurs near the base of the hills and fog forms there. As drainage continues, the mixing process persists and the depth of the fog increases. As the ratio of cold air from the hillside (point B) to the somewhat warmer valley air (point A) increases more water is made available for condensation on cloud nuclei and widespread fog develops. Near the fog base, the drops are large and the LWC is high, but the concentration of droplets is depleted because of sedimentation and fallout.

Near the fog top continued radiational cooling of the air results in slight supersaturation and additional fog formation. The continuous formation of new droplets with negligible terminal velocities accounts for the observed high concentration of small droplets near the fog top.

Although other explanations of the manner in which fog forms at the valley site may be plausible, most of our observations suggest that the above reasoning is valid. It is obvious, however, that many additional measurements of the microphysical features of the fog would be needed to define how these changes take place with time. At the present time we are modeling the fog formation process in the computer by assuming various observed nucleus size spectra and producing fog by continuous cooling and also mixing. The results of these studies will be reported in a subsequent report.

C. Fog Seeding Results - Ground Seeding

As previously stated, fog seeding experiments were initially performed employing ground based seeding apparatus. A total of 25 ground seeding experiments were conducted, most of which resulted in some observed improvement in visibility. In more than half of the experiments the seeded air mass passed between the instrumentation sites and consequently quantitative data could not be taken. In spite of this difficulty, several reasonably successful seeding experiments were performed in which detailed information was obtained on fog characteristics. Experiments in which a noticeable visibility improvement occurred in the seeded area are typified by results presented below. In this experiment (8 September 1968) the seeded area passed over one of our transmissometers as observations of drop size were being made. Detailed analysis of the relationships between drop sizes, visibility and liquid water content of the fog could therefore be made.

Prior to seeding, the CAL Aztec obtained data on fog characteristics. Fog had formed in the valley about 4:30 a.m. and by 5 a.m. airport ground conditions were WOXOF. Following take-off, (6:30 a.m.) the airborne observer reported fog depth to be 100 m. Visibility at the ground was about 100 m and fog liquid water content was 170 mg m^{-3} . Wind velocity was three knots at 260° .

Our initial plan was to seed the fog with 280 lbs of sized NaCl* (5-20 μ diameter) at a dissemination rate of about 30 lbs/min. The instrumented van was positioned a short distance from the seeding rig so that drop size data could be collected in the unmodified fog and in the seeded area as the plume moved downwind. Shortly after seeding was started, however, a 60 $^{\circ}$ shift in wind caused the salt plume to drift away from our instrumentation and the airport. The experiment was, therefore, terminated after four minutes of seeding (\sim 130 lbs of material were expended) and the rig was moved to a more favorable location.

The position of the seeding unit for the second experiment is shown in Figure 5 (the original location of the seeding rig was on the approach end of Runway 10). Also shown in the figure are the locations of transmissometers used in this experiment. The distance from the seeding unit to transmissometer (1) is 0.83 mile.

Seeding with the remaining 150 lbs of material was scheduled for 7:25 a.m. Fog density and liquid water content had not changed appreciably during the previous hour. Based on the wind direction and speed (240 $^{\circ}$ at 6 knots) we predicted that particles injected into the fog in the vicinity of Taxiway B would reside in the foggy air approximately 9 minutes before reaching the opposite end of the airport. According to our model, this would be ample time for the salt to have a significant effect on the natural drop size distribution.

Seeding was started at 7:25 a.m. and completed at 7:30 a.m. The 30 lb/min dissemination rate was intended to provide approximately 3 mg of NaCl particles per cubic meter of treated fog. Droplet data obtained by ground observers indicated that the salt plume followed a path similar to that shown in Figure 5. Visibility measurements obtained with transmissometer (1) indicate that visibility increased from about 300' to about 820' between 7:30 and 7:42 a.m. No other transmissometer indicated any change in visibility during the same period of time. The improvement in visibility by a

*Particle sizing done by Meteorology Research, Inc., Altadena, Calif.

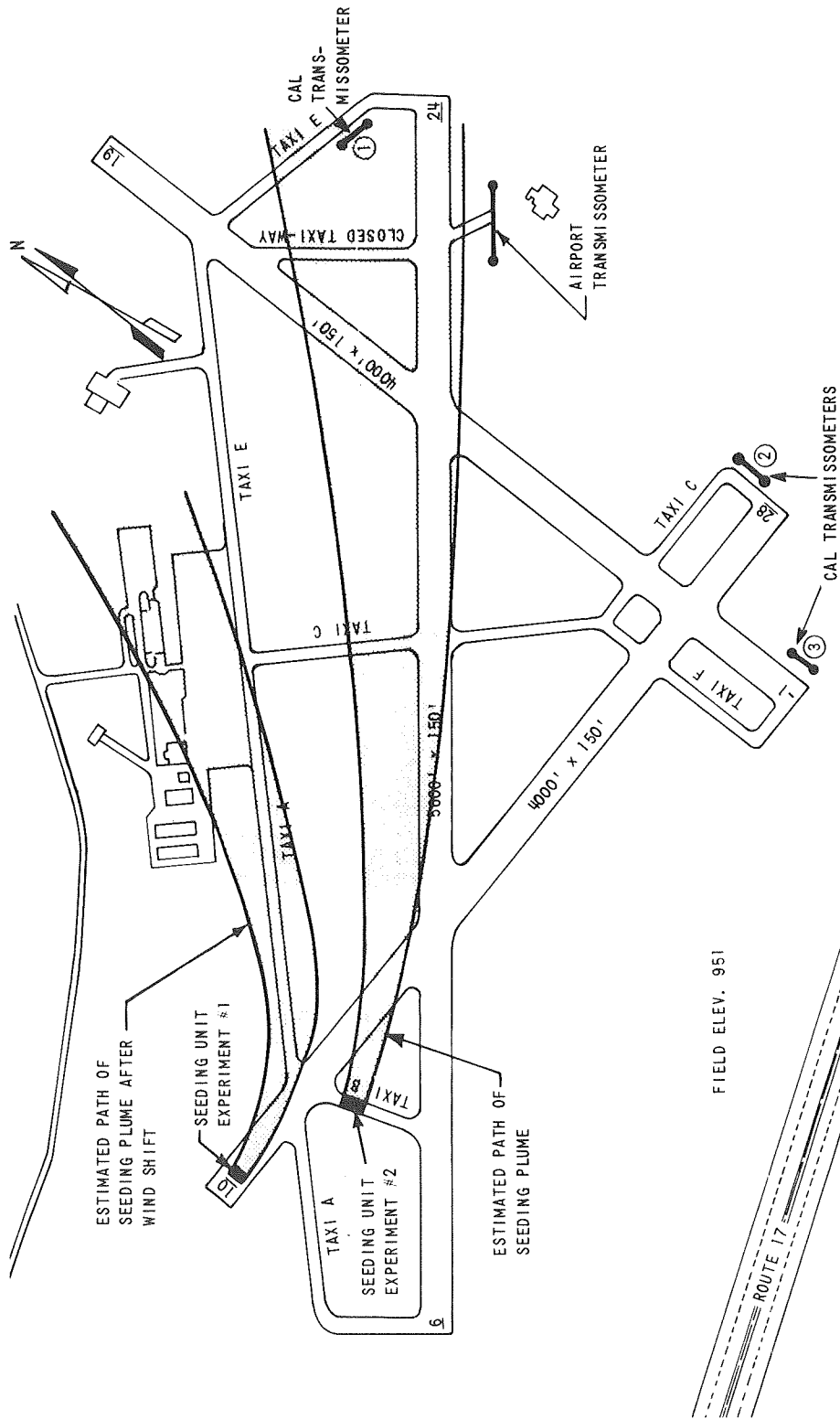


Figure 5 LOCATION OF SEEDING UNIT AND TRANSMISSOMETERS AT EXPERIMENTAL FIELD SITE -
CHEMUNG COUNTY AIRPORT, ELMIRA, NEW YORK, SEPTEMBER 8, 1968

factor of 2.5 to 3.0 is typical of the results obtained in most ground seeding experiments.

Because of the large average drop sizes in the natural fog, the expected visibility improvement was less than we originally predicted. For example, seeding a fog consisting of 5μ radius drops with 10μ radius dry hygroscopic particles could be expected to give a ten-fold increase in visibility, according to our model. Seeding a fog consisting of 9μ radius drops, using the same material, could only be expected to give a six-fold increase in visibility due to changes in drop size.

Figure 6 shows the drop size distribution obtained in the seeded portion of the fog at about 7:40 a.m. The data were collected alongside transmissometer (1). A drop distribution from the adjacent unmodified fog, taken a few minutes earlier, is shown for comparison. As shown, a significant change had occurred in the drop sizes after seeding. Also shown in the legend of the figure are the computed drop concentrations, liquid water contents and mean volume diameters for the seeded and unseeded fogs. It is perhaps interesting to note that the liquid water content was higher in the seeded region than in the natural fog. All visibility improvement at the time of these measurements therefore resulted from a favorable shift in drop size distribution.

Variations in the calculated liquid water content can be expected, of course, depending on whether large saline droplets are encountered when the sampling is taken. It is frequently difficult to obtain statistically valid drop size distributions, particularly in seeded fog where drop concentrations are low. In spite of these difficulties the data suggest that after seeding, the relative humidity was initially lowered by a few percent, an occurrence which is expected from theory and commonly noted in laboratory experiments. Somewhat later in time, after most of the largest drops settled out of the fog, visibility improvements greater than those measured probably occurred but instrumentation was not suitably located for observation further downstream.

Results from early tests demonstrated that seeding from the ground, using sized hygroscopic nuclei, can be effective in producing visibility

improvements. Although ground based seeding did not improve visibility above the landing minimums, the nearly three-fold increase in visual range was encouraging. The principal problem seemed to be that of effectively distributing the seeding material throughout the fog volume. Mixing of unmodified fog with the narrow seeded region from a single seeding unit frequently limited the visibility improvement that could be achieved. Improved methods of particle dissemination must be sought if the ground system is to be adapted to airport use. These limitations prompted us to test aircraft seeding techniques during the latter part of the experimental period.

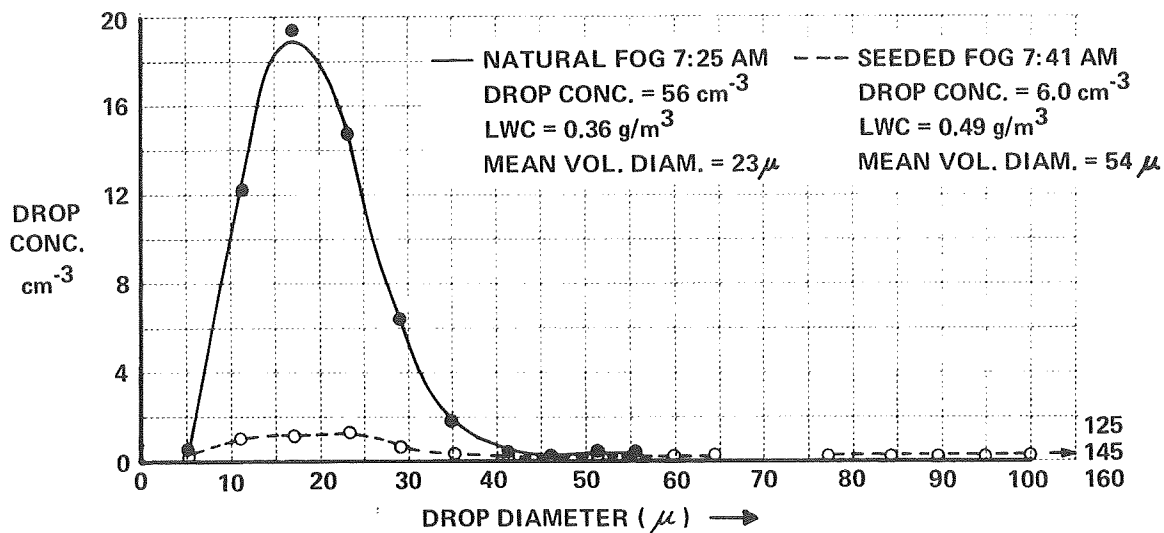


Figure 6 COMPARISON OF DROP SIZE DISTRIBUTIONS FOR NATURAL AND SEEDED FOG, SEPT. 8, 68

D. Fog Seeding Results - Aerial Seeding

Aerial seedings of dense valley fog were performed during the first three weeks in October 1968. A Piper Pawnee aircraft, designed for crop dusting, was obtained for the experiments.* A total of six seeding trials were conducted using various aerial seeding methods. Our plan was to seed the fog a prescribed distance upwind of the airport (depending on wind speed

* Rented from EG&G, Boulder, Colorado.

and direction) and allow the seeded area to drift over the ground instrumentation located near the runways.

On two occasions spiral seeding over the fog top was attempted but difficulties in maintaining the prescribed flight pattern resulted in ineffective seeding. The procedure that produced the most outstanding results involved flying perpendicular to the prevailing wind and disseminating dry particles in "evenly" spaced rows over the fog top. For these experiments the volume to be cleared of fog was approximately $3 \times 10^7 \text{ m}^3$. The results of one seeding trial (16 October 1968) are discussed below in some detail. In this experiment a significant amount of data were collected, both in seeded and unmodified fog.

Prior to seeding, routine procedures were followed in collecting data on fog characteristics. Fog depth was reported as 350 ft with a layer of haze exceeding 1000 ft lying above the fog top. Horizontal visibility measured 300 ft; liquid water content was about 280 mg m^{-3} . Representative drop size distributions at four different levels in the fog prior to seeding are shown in Figure 7. Note the differences in drop concentration and size near the fog top as compared to the values near the base.

Seeding was accomplished with approximately 700 lbs of NaCl^* having a size range of 10-30 μ diameter. The aircraft completed seeding of the fog top in about 7 minutes, traversing an area approximately 1/2 mile by 1/4 mile. The salt concentration within the fog was therefore about 40 mg m^{-3} . Three photos taken during various stages of the experiment are shown in Figure 8. Note, in the second photo the seeding aircraft and trailing salt plume. Within a few minutes after seeding, narrow paths began to open in the fog, increasing in size until, after 15 minutes, large areas of the fog were completely dissipated. (Visibility in the seeded area improved to approximately 1/2 mile.) The cleared region persisted for about 15 additional minutes before unmodified fog began to encroach into the seeded region and reduce visibility.

*Sized material purchased from Meteorology Research, Inc., Altadena, Calif.

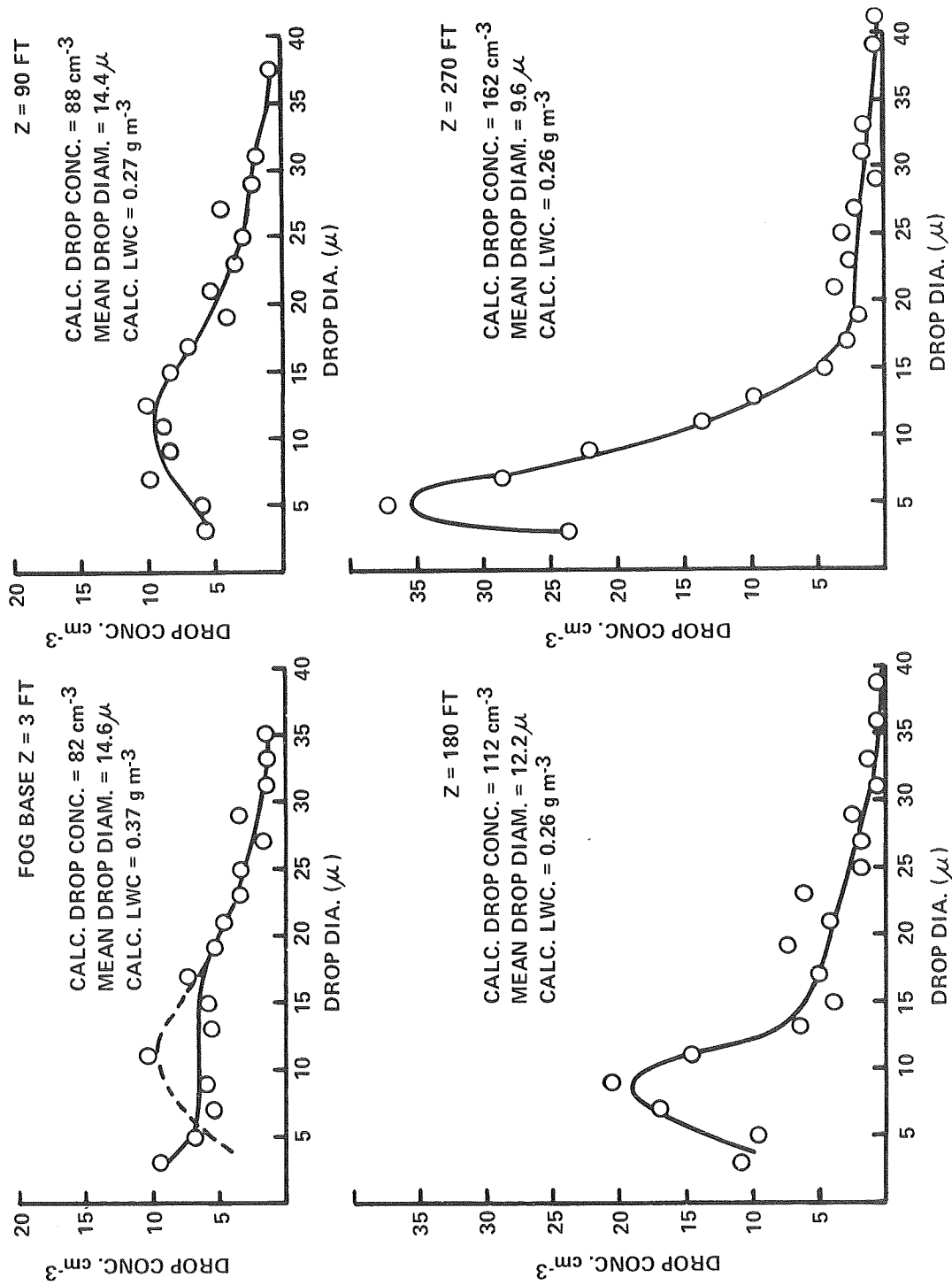
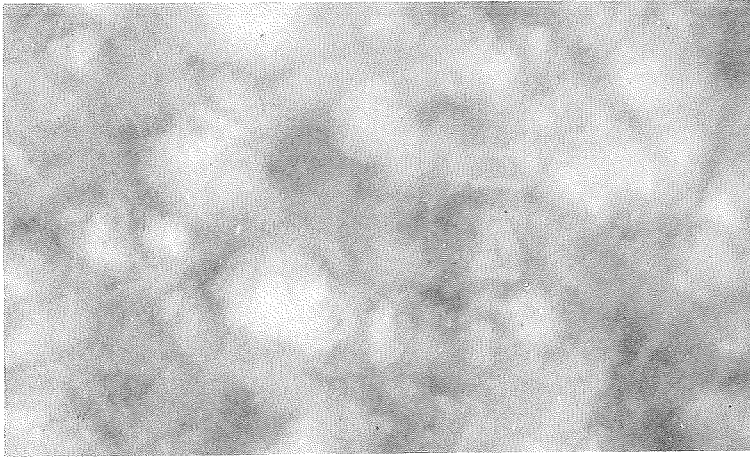
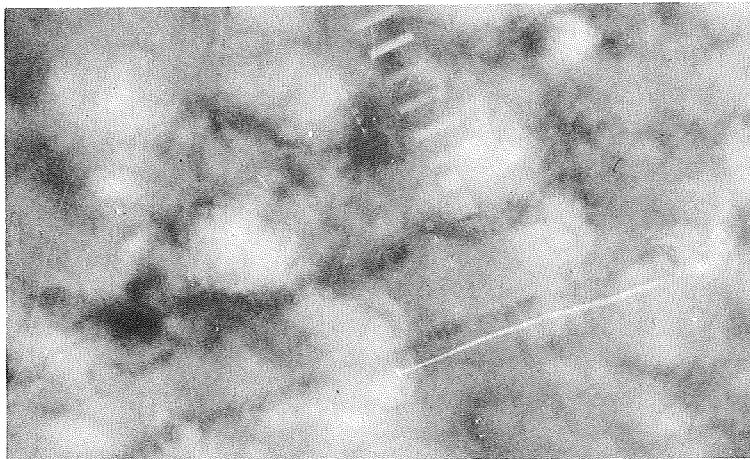


Figure 7 DROP SIZE DISTRIBUTIONS AT FOUR LEVELS IN A VALLEY FOG
 PRIOR TO SEEDING - ELMIRA, NEW YORK, 16 OCTOBER 1968

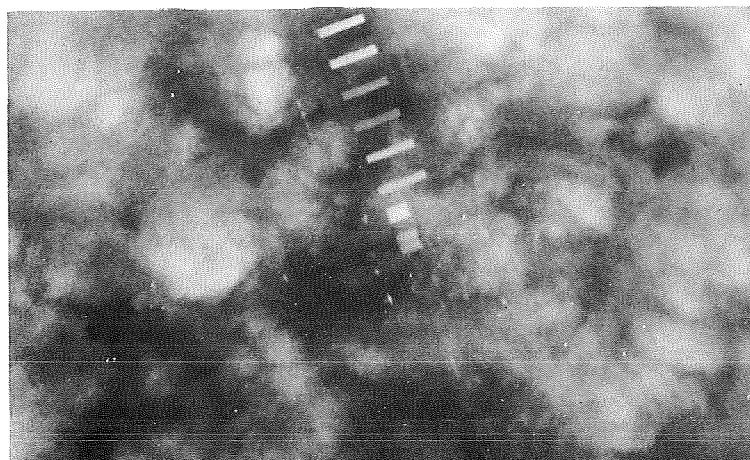
**FOG TOP VIEW FROM AN
ALTITUDE OF 10,000 FEET. NOTE
THE HANGARS (200 FEET LONG)
AND AIRCRAFT ON THE GROUND
AFTER SEEDING.**



**TARGET AREA ONE MINUTE
PRIOR TO SEEDING.**



**THE TARGET AREA DURING
SEEDING (SALT PLUME AND
SEEDING AIRCRAFT ARE
VISIBLE).**



**THE TARGET AREA 15 MINUTES
AFTER START OF SEEDING.**

Figure 8 THREE PHOTO SEQUENCE OF FOG CLEARING

Figure 9 shows a comparison of drop size distributions for the seeded and natural fogs. The curves represent data taken approximately one minute before seeding began and again approximately nine minutes after seeding had started. Tabulated in the legend of the figure are several fog parameters as determined from the data. Note the rather dramatic shift in the drop size distribution after seeding. It is apparent from the data that the seeded fog was comprised of fewer droplets having somewhat large size. Accompanying the shift in drop sizes for the data shown was a decrease in liquid water content of the fog due to sedimentation of the largest saline drops. The combined effects of drop size differences and liquid water changes were responsible for the visibility improvements that occurred. Analysis of data has indicated that approximately 60% of the visibility improvement was accounted for by the decrease in fog liquid water caused by precipitation of the large saline droplets after seeding.

E. Conclusions from 1968 Field Experiments

These experiments have demonstrated the validity of a concept for improving visibility in dense natural fogs by seeding with sized hygroscopic particles. Data analysis has shown that the initial visibility improvement in seeded fog is the result of a favorable shift in the drop size distribution (even though liquid water content is temporarily increased). Subsequent improvement in visibility is due to a reduction in liquid water content associated with precipitation of large saline droplets formed on artificial nuclei.

Airborne seeding experiments were most effective in causing fog dissipation. In the ground seeding experiments, it is likely that mixing of unmodified fog into the narrow seeded region limited the visibility improvements that occurred. Multiple seeding passes with the aircraft enabled us to treat a much wider volume of fog and minimized the effects of mixing.

Several problems still exist. In most cases it was apparent in both airborne and ground based seeding experiments that a substantial amount of clumping of seeding material had occurred. Thus, the efficiency of the seeding material was substantially reduced. More effective methods for particle dissemination must be devised.

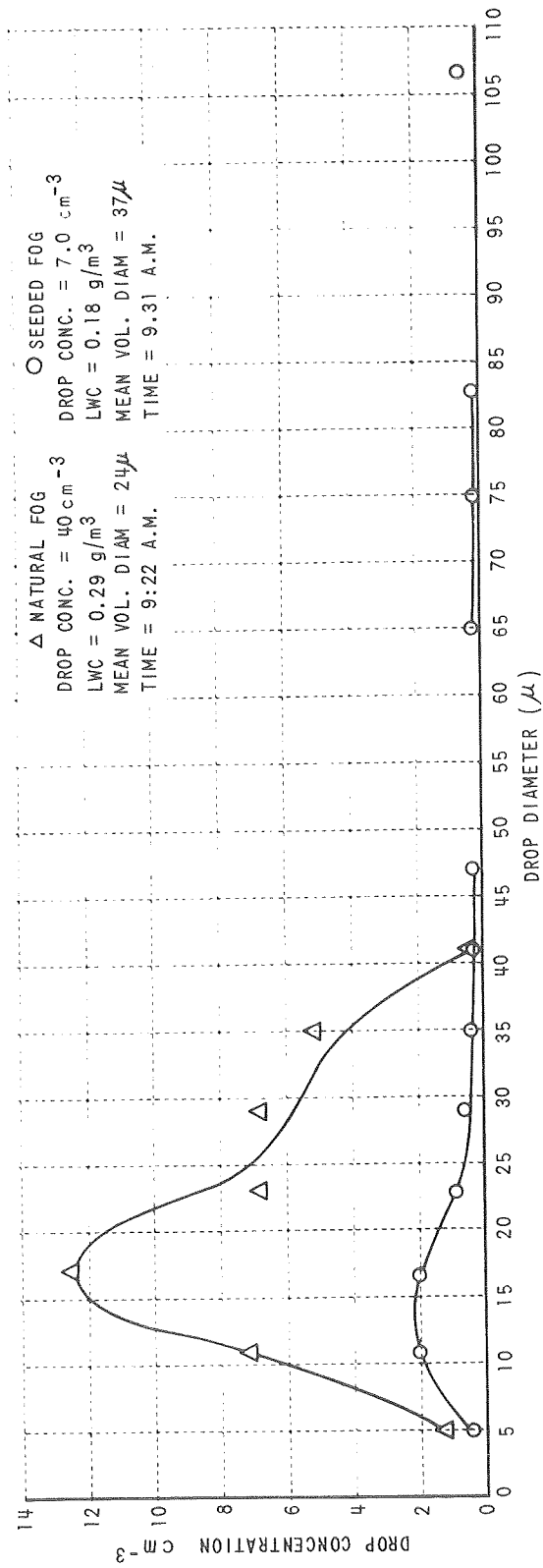


Figure 9 COMPARISON OF DROP SIZE DISTRIBUTIONS FOR SEEDED AND UNSEEDED NATURAL FOG
 ELMIRA, N.Y. 10/16/68

An equally important problem is that of selecting and testing non-corrosive, ecologically safe chemicals to replace NaCl as the seeding material. Laboratory experiments have shown that several hygroscopic materials are almost as effective as salt for fog dispersal. Additional work leading to the selection of more suitable seeding agents is now under way. Field evaluation of one or two of the most promising materials is one of the objectives of next year's research.

III. COMPUTER MODELING

A computer model has been developed to simulate the response of natural and artificial fogs to seeding with hygroscopic nuclei. The theoretical principles of warm fog modification with sized hygroscopic nuclei as discussed by Pilié et al. (1967) and Jiusto et al. (1968) form the basis of the computer model. The computer model, however, permits the elimination of certain simplifying assumptions that were employed in earlier analytic treatments. More important, the model allows the detailed investigation of the influences of such seeding variables as: a) the properties and structure of the fog prior to seeding, b) the chemical properties, size distribution, and amount of seeding material employed, and c) the method of dispensing the seeding material into the fog. In addition, the model has been used to study the role of atmospheric turbulence in dispersing the seeding material and mixing unmodified with modified fog.

The primary emphasis in the development of the present computer model has been placed on the support and guidance of the field experimentation portion of this program. Thus, there has been no hesitancy to employ appropriate approximations and simplifications in the model, at the expense of some rigor and sophistication, in order to achieve a computer model which is capable of simulating the essential features of a great number of different modification experiments without entailing prohibitively large computational requirements.

It is important to emphasize the two-way exchange of information between the field experimentation program and the computer modeling work on Project Fog Drops, an exchange that has contributed to the improvement and success of both phases of the project. The field experimentation program provided detailed data on the properties of the valley fogs at the experimental site (including drop-size distribution, liquid water content, visibility, wind, temperature, vertical structure and condensation nucleus measurements), which are necessary

inputs if the computer model is to provide meaningful simulations of seeding effects. The computer model, in turn, provided information on the seeding rates required to produce significant clearing under various conditions and the times required for this clearing to be effected.

A. Description of the Basic Model

In a mathematical sense, the computer model integrates numerically a system of ordinary, first order, differential equations which describe the growth and sedimentation of the solution drops that form on the particles of hygroscopic seeding material, the accompanying reduction in relative humidity, and the resulting evaporation of the natural fog drops. The results of seeding are assessed by periodically computing and printing out several variables such as the horizontal and vertical visibility, the drop-size distribution, liquid water content, and relative humidity.

In order to model the effects of the sedimentation of solution drops and provide an accurate description of the vertical variation of visibility and other fog properties, the effects of seeding are computed at several equally spaced vertical levels in a model fog. An initial supersaturation, size distribution of fog drops, and cooling rate (if any) is specified for each of the vertical levels at the beginning of a simulation. In addition, the chemical properties and size of the condensation nuclei upon which the fog drops are assumed to be formed must also be specified. The initial size distribution of the fog drops determines the liquid water content and visibility in the model fog prior to seeding.

To simulate the dispensing of the seeding material into the fog, an initial size distribution of hygroscopic seeding material is assumed to be injected at the start of a simulation at one or more of the vertical levels in the model fog.

The size distributions of fog drops and of seeding material, and hence of solution drops that form on the particles of hygroscopic seeding material, are approximated in the model by discrete classes. For each

class, k , of fog or solution drops in the model, there is a differential equation for the diffusional growth of the drops of form (Fletcher, 1962)

$$\frac{dr_k}{dt} = \frac{G}{r_k} \left(S - \frac{A}{r_k} + \frac{B_k}{r_k^3} \right) \quad (1)$$

where the time rate of change of the drop radius r_k depends upon the local supersaturation S and the magnitude of r_k . The solution constant B_k is given by

$$B_k = 4.3 \frac{i_k m_k}{M_k} \quad (2)$$

where i_k is the van't Hoff dissociation factor, M_k is the molecular weight and m_k is the mass of the nucleus upon which the drop was formed. The growth constant G and surface tension constant A are treated as functions of the initial environmental temperature only.

By employing an approximate form of the diffusional growth equation which is accurate for dilute solutions only (see discussion by Low, 1969), at all concentrations, appreciable errors are incurred in computing the initial growth of the solution drops which form on the seeding nuclei. Fortunately, in most of the seeding situations investigated with this model, the initial deliquescence and growth of the solution drops is so rapid compared with their sedimentation rate, that little error is introduced. Errors of a similar origin, that arise when the natural fog drops are almost completely evaporated, such at the top of the model fog when simulating aerial seeding, generally do not have a significant effect on the computed vertical visibility since this quantity is principally determined by more modest clearings produced elsewhere.

Because of the unresolved questions recently raised by Aroesty and Koenig (1969) concerning the proper ventilation correction for small droplets, the effect of ventilation on drop growth has been neglected in the present model. Coalescence between the falling solution drops and the natural fog drops, an important factor in the modification of deep fogs and stratus decks, has been neglected in this model.

For each of the equally spaced vertical levels, j , in the model, the time rate of change of the supersaturation S_j at that level is computed from the approximate relation

$$\frac{dS_j}{dt} = +C_1 \frac{dT_j}{dt} - C_2 \frac{dm_j}{dt} \quad (3)$$

where $\frac{dT_j}{dt}$ is an externally imposed cooling rate (if any) and $\frac{dm_j}{dt}$ is the net rate of condensation per unit volume at that level. The constants C_1 and C_2 are treated as a function of the initial environmental temperature only and are given by

$$C_1 = \frac{LM_o}{RT^2} \quad (4)$$

and

$$C_2 = \frac{L^2 M_o}{TPM_a C_p} + \frac{RT}{e_s M_o} \quad (5)$$

where T is the absolute temperature, R is the ideal gas constant, L is the latent heat of condensation, P is the total atmospheric pressure, C_p is the specific heat of air at constant pressure, M_a is the average molecular weight of air, e_s is the saturation vapor pressure of water vapor and M_o is its molecular weight. The release of latent heat of condensation and the extraction of water vapor from the atmosphere are both accounted for in the derivation of the expression for C_2 by Squires (1952). The expression for C_1 was obtained from the Clausius-Calpeyron equation.

The approximations involved in Equation (3) are such that it is an exact relation at water saturation or when $S = 0$, but it becomes increasingly less accurate as conditions depart from saturation. For a reduction in relative humidity of 10% or $S = -0.1$, however, the error in the computed value of S resulting from the application of Equation (3) is only of order $+0.005$. In most of the seeding situations investigated with the computer model, the relative humidity reductions were considerably less than

10% and Eq. (3) was a very good approximation. The only exceptions were simulations of aerial seedings in which excessive amounts of seeding material were used. In these cases the relative humidity reductions near the top of the fog approached the relative humidity reduction over a saturated solution of the seeding material.

It should be noted that the provision for externally imposed isobaric cooling in the model permits the simulation of the processes of fog formation on a population of condensation nuclei under the influence of radiational cooling.

The change of height h_k for each class, k , of solution drops in the model is computed from the equation

$$\frac{dh_k}{dt} = -W(r_k) \quad (6)$$

where $W(r_k)$ is the instantaneous terminal velocity of the drops in that class. The terminal velocities of the solution drops are computed from the Stokes relation for drops of less than 25 microns radius and from a more general empirical function (Best, 1950) for drops of radius greater than 25 microns.

The effects of the sedimentation and fallout of the solution drops which form on the particles of hygroscopic seeding material are modeled by a method similar to that employed by Mordy (1959) in studying condensation in an updraft. The instantaneous value of the local supersaturation S_j governing the growth [Eq. (1)] of a given class of solution drops falling between two of the vertical grid levels is determined by linear interpolation between the instantaneous supersaturations at the immediately adjacent upper and lower grid levels. Similarly, the rate of condensation on that class of solution drops is linearly apportioned to the net condensation rates [Eq. (3)] at the immediately adjacent upper and lower grid levels according to the relative position of the class between the grid levels.

Sedimentation of the fog drops (which is relatively slow) is neglected in the present model. Consequently, the various classes of fog drops evaporate under the influence of the supersaturation S_j at their original level, j , and, in turn, contribute to reduction of the net condensation rate $\frac{dm_j}{dt}$ at that level.

In the computer model, this system of coupled differential equations is integrated numerically by means of a variable-time step, fourth-order predictor-corrector routine to establish the temporal evolution of supersaturation, size distributions of fog and solution drops, and related fog properties such as the visibility and liquid water content. In order to eliminate the necessity of prohibitively small time steps to maintain a stable integration when the fog drops have evaporated to small sizes, the radius of a class of fog drops is equated to the equilibrium radius at the prevailing supersaturation whenever the radius falls below some limiting radius, typically taken as one or two microns. This is possible because drops of this size respond very rapidly to changes in supersaturation (see curves for drop evaporation given by Kocmond and Jiusto, 1967).

The horizontal visibility V_j at each vertical level, j , in the model fog is evaluated from the standard expression for the meteorological visual range in uniform fog of large water droplets (Middleton, 1952)

$$V_j = \frac{3.912}{\sigma_j} = \frac{3.912}{2\pi \sum N_k r_k^2} \quad (7)$$

where the summation of contributions to the extinction coefficient σ_j extends over all classes of fog drops at that level and the linearly apportioned contributions of all classes of solution drops lying between that level and the immediately adjacent vertical levels. The liquid water content at each vertical level is computed through a similar procedure.

The vertical visibility through the model fog is computed from the expression

$$V = \frac{3.912 H}{\int_0^H \sigma dz} \quad (8)$$

where the integral of the extinction coefficient from the bottom of the fog to the top of fog H is evaluated by Newton-Cotes numerical integration over the computed values of the extinction coefficient at the equally spaced vertical levels in the model fog.

B. Modeling of the Effects of Turbulent Diffusion

In order to investigate the influences of atmospheric turbulence upon warm fog modification with sized hygroscopic nuclei, the basic computer model has been modified to permit the simulation of the effects of horizontal turbulent diffusion on the modification produced by continuous point sources and instantaneous line sources of seeding material. The continuous point source modification of the model is employed to simulate seeding from a single ground-based disseminator, while the instantaneous line source is an idealization of a trail of seeding material disseminated on the top of a fog by an aircraft.

The effects of turbulent diffusion in the vertical have been neglected in the present model, principally because of far greater computational problems involved in their simulation. In stable situations, at least where vertical diffusion is greatly suppressed (Lumley and Panofsky, 1964; Turner, 1969), the influences of vertical diffusion upon fog modification are likely to be almost negligible. In near-neutral situations, which are typical of the Elmira valley fog, vertical diffusion may have significant effects on the distribution of clearing in the vertical; however, horizontal diffusion remains a more important factor in controlling the regrowth of fog in a cleared zone.

The simulation of the effects of horizontal diffusion is based on the widely used Gaussian model (see Turner, 1969) of turbulent diffusion. The number concentration of solution drops produced by a continuous point seeding source is given by

$$C_p = \frac{Q_p e^{-\frac{1}{2} \left[\frac{Y}{\sigma_y(X)} \right]^2}}{\sqrt{2\pi} U D \sigma_y(X)} \quad (9)$$

where Q_p is the seeding source strength in number of particles per unit time, U is the mean wind speed, D is the vertical depth of the region influenced, X is the distance downwind from the point source, Y is the cross-wind distance from the centerline of the Gaussian distribution, and $\sigma_y(X)$ is the standard deviation of Gaussian distribution in the cross-wind direction. Similarly the number concentration of solution drops produced by

an instantaneous line seeding source is given by

$$C_L = \frac{Q_L e^{-\frac{1}{2} \left[\frac{Y}{\sigma_y(X)} \right]^2}}{\sqrt{2\pi} D \sigma_y(X)} \quad (10)$$

where Q_L is the seeding source strength in number of particles per unit length, Y is the cross line distance from the center of mass of the distribution, $\sigma_y(X)$ is the standard deviation of the Gaussian distribution in the cross line direction, $X = Ut$ is the downwind distance since the generation of the instantaneous line source at time $t = 0$, and the other symbols are as defined above.

In order to minimize computational requirements, the computer model is presently restricted to computing the fog modification produced at the centerline of modified region where the modification is at a maximum. Setting $Y = 0$ and $X = Ut$ in Eq. (9) and Eq. (10), the resulting expressions are applied to each class of solution drops in the model to compute the time variation of the number concentration of drops in that class at the centerline of Gaussian distribution.

Turbulent diffusion not only disperses the solution drops which form on the particles of hygroscopic seeding material, but it also causes a regrowth of fog in a modified region through mixing. Since the modification of a warm fog by seeding with hygroscopic nuclei depends upon a reduction in supersaturation and evaporation of the fog drops, it is necessary to model the influence of turbulent diffusion on both the supersaturation and fog drop size distribution. This is accomplished in the present model by noting that on the centerline of the Gaussian distribution, Eqs. (9) and (10) can be written in the form

$$\frac{dC}{dt} = -C \frac{d \ln [\sigma_y(Ut)]}{dt} \quad (11)$$

where the time rate of change of the concentration C depends upon the product of instantaneous value of concentration and a single turbulence dependent derivative. It is assumed in the computer model that this form of time dependence can be generalized to represent the influence of horizontal diffusion

on the supersaturation and fog drop size distribution at the centerline of the modified region.

For each discrete class of fog drops, k , in the model, it is assumed that a change in size produced by turbulent diffusion alone is given by

$$\frac{d \Delta M_k}{dt} = -\Delta M_k \frac{d \ln [\sigma_y (Ut)]}{dt} \quad (12)$$

where $\Delta M_k = r_{k_0}^3 - r_k^3$ is proportional to the mass deficit between the unmodified fog drops of radius r_{k_0} at $Y = \pm \infty$ and the fog drops of radius r_k at the centerline of the modified region. The number concentration of fog drops in each class is everywhere uniform at its value in the unmodified fog, and hence is unchanged by turbulent diffusion. Substituting for ΔM_k in Eq. (12) and differentiating, it can be shown that the time rate of change of r_k produced by turbulent diffusion alone is

$$\frac{dr_k}{dt} = \frac{(r_{k_0}^3 - r_k^3)}{3 r_k^2} \frac{d \ln [\sigma_y (Ut)]}{dt} \quad (13)$$

In the computer model, this turbulence contribution is added to the contribution from diffusional growth or evaporation [Eq. (1)] to obtain a differential equation for the combined influence of diffusional growth and turbulence on the radius of the fog drops at the centerline of the modified region.

Similarly, for each vertical level, j , in the model, it is assumed that a change in the supersaturation S_j produced by turbulent diffusion alone is given by

$$\frac{d \Delta S_j}{dt} = -\Delta S_j \frac{d \ln [\sigma_y (Ut)]}{dt} \quad (14)$$

where $\Delta S_j = S_{j_0} - S_j$ is the supersaturation deficit between the unmodified supersaturation S_{j_0} at $Y = \pm \infty$ and the supersaturation S_j at centerline of the modified region. Substituting for ΔS_j in Eq. (14), we obtain an expression

$$\frac{d S_j}{dt} = (S_{j_0} - S_j) \frac{d \ln [\sigma_y (Ut)]}{dt} \quad (15)$$

for the turbulence contribution which is added to the diffusional growth contribution [Eq. (3)] to obtain a differential equation for the combined influence of diffusional growth and turbulence on the supersaturation S_j at the center-line of the modified region.

It is important to note that from Eq. (3), in the absence of external cooling, ΔS_j is equal to $C_2 \Delta m_j$ where Δm_j is the net condensation per unit volume or the net mass deficit of water vapor per unit volume. Thus, the turbulent transport of ΔS_j expressed in Eq. (14) is equivalent to a turbulent transport of the mass deficit of water vapor per unit volume, and is required to conserve total water content in the simulation of the effects of turbulent diffusion. It has, in fact, been verified in numerous different integrations of the combined system of differential equations discussed above that, prior to the fallout of any solution drops at the bottom of the model fog, the total water content in a vertical column of the model fog is invariant under the simulation of the influences of turbulent diffusion on fog modification.

While this approach to the modeling of the effects of turbulence permits any function form of $\sigma_y(x) = \sigma_y(Ut)$, the simple power law (Cramer et al., 1964)

$$\sigma_y(Ut) = \sigma_{y_0} \left(\frac{X_0 + Ut}{X_0} \right)^P \quad (16)$$

has been employed in all of the seeding situations investigated with the computer model. Here σ_{y_0} is an assumed initial standard deviation of the distribution of seeding material and X_0 is a virtual downwind distance corresponding to σ_{y_0} . In this case, the turbulence related derivative appearing in Eqs. (11) through (15) assumes the simple form

$$\frac{d \ln [\sigma_y(Ut)]}{dt} = \frac{PU}{X_0 + Ut} \quad (17)$$

In simulations of ground-based seedings using the continuous point source mode of the computer model, the empirical curves of Cramer et al. (1964) and Turner (1969) have been employed to estimate the virtual distance X_0 corresponding to an assumed value of σ_{y_0} and the power law exponent P under various stability conditions.

Simulations of aerial seedings using the instantaneous line source mode of the computer model, have been based on the Smith and Hay (1961) description of the expansion of clusters of particles in which

$$\frac{d\sigma_y(x)}{dx} \approx 3i^2 \quad (18)$$

where $i = \frac{\sqrt{u^2}}{U}$ is the intensity of turbulence. Under this approximation, the power law exponent P in Eq. (16) is unity and the virtual distance $x_0 = \sigma_{y0} / 3i^2$.

While the value $i = 0.1$ appears to be a reasonable value in near-neutral situations, there is little information on appropriate values of i for the modeling of diffusion in stable situations, particularly under low wind conditions where large, low frequency variations in wind direction may be important (Smith and Abbott, 1964; Lumley and Panofsky, 1964). Based on some data for turbulent dispersion for instantaneous sources (Turner, 1969), the value $i = 0.05$ has been employed in the model to simulate diffusion in very stable situations. From Eq. (18), this corresponds to an expansion rate of approximately one quarter the expansion rate under near-neutral conditions.

C. Results

The computer model has been employed to simulate the fog modification produced in a large number of seeding situations. The efficiency of various size distributions and amounts of both NaCl and urea in modifying valley fogs has been studied for both aerial and ground-based seeding.

To provide a concrete example of the use of the basic computer model without the effects of turbulent diffusion, a simulation of an actual aerial seeding experiment will be discussed in some detail. In this experiment on October 16, 1968, 700 lbs of NaCl having a size range of 10-30 μ diameter were dispensed over a 1/2 mile by 1/4 mile area at the top of a 100 meter deep fog. Substantial clearing was produced in the seeded region with the horizontal visibility at the surface increasing from approximately 100 m just before seeding to 800 m (\sim 1/2 mile) 15 minutes after the start of seeding.

In the computer simulation of this experiment, the size distribution of the fog drops obtained just prior to seeding was approximated by the discrete size distribution shown in Figure 10. The fog properties computed from this discrete size distribution are almost identical to those measured in the actual fog. For simplicity, it was assumed that this initial fog drop distribution applied throughout the 100 m depth of the fog, thereby neglecting any variation in the properties of the natural fog with height. The properties of the condensation nuclei upon which the various size classes of fog drops were assumed to be formed were deduced from condensation nuclei measurements at the experimental site. The fog temperature was assumed to be 10° C.

The 10-30 μ diameter size distribution of the NaCl seeding material was approximated by the discrete size distribution shown in Figure 11. In the computer simulation, the effects of dispensing various amounts of this size distribution of NaCl particles on the top of the fog were calculated at the 0, 50, and 100 m levels in the model fog. The results are shown in Figure 12, where computed curves of horizontal visibility vs. height in fog are plotted as a function seeding rate and time after deposition of the NaCl at the top of the fog. The 120 m visibility in the model fog before seeding is indicated by the vertical line for time equal zero.

Examining the general height dependence of the computed visibility, we see a decrease in the effectiveness of seeding with distance from the top of the fog. Because of this decrease, it may be necessary to rely on coalescence between the solution drops and the fog drops as the main mechanism for effecting a modification of the lower layers of stratus decks and deep fogs when seeding from above by aircraft.

The 1.0 g m^{-2} concentration of NaCl on the top of the fog corresponds to the average concentration of seeding material dispensed in the experiment, but, since the distribution of seeding material on the top of the fog was not entirely uniform, curves for one half and twice the average concentration are also shown.

After 20 minutes, in the case of 0.5 g m^{-2} concentration of NaCl, all of the solution drops which formed on the NaCl particles had fallen out of

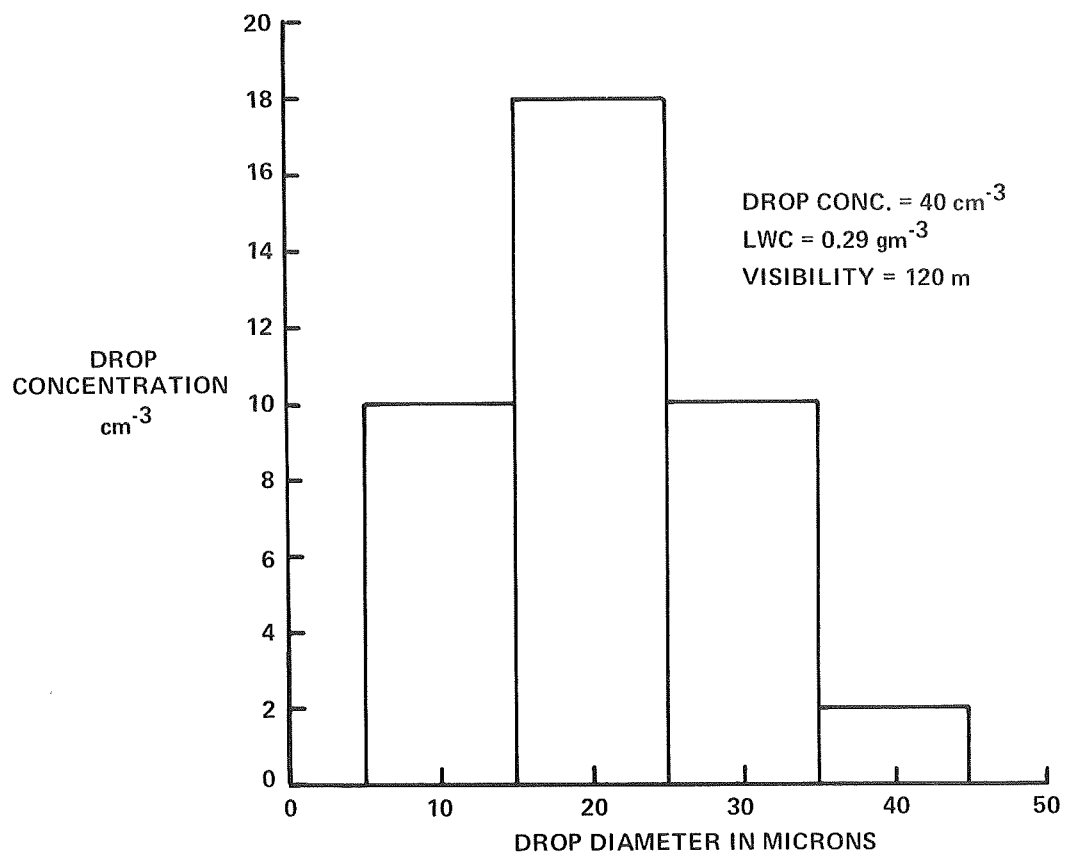


Figure 10 FOG DROP DISTRIBUTION USED IN COMPUTER SIMULATION OF FOG SEEDING BY AIRCRAFT

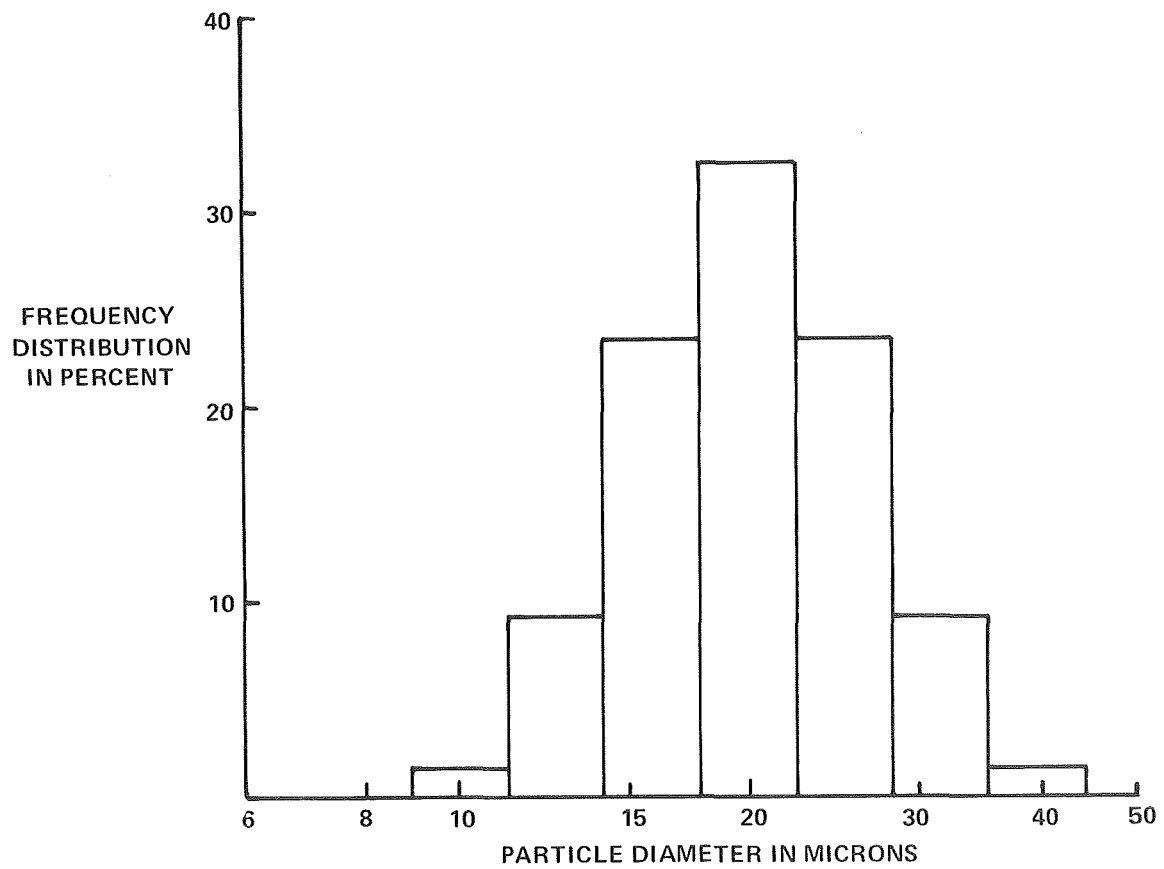


Figure 11 SIZE DISTRIBUTION OF NaCl SEEDING MATERIAL USED IN COMPUTER SIMULATION OF FOG SEEDING BY AIRCRAFT

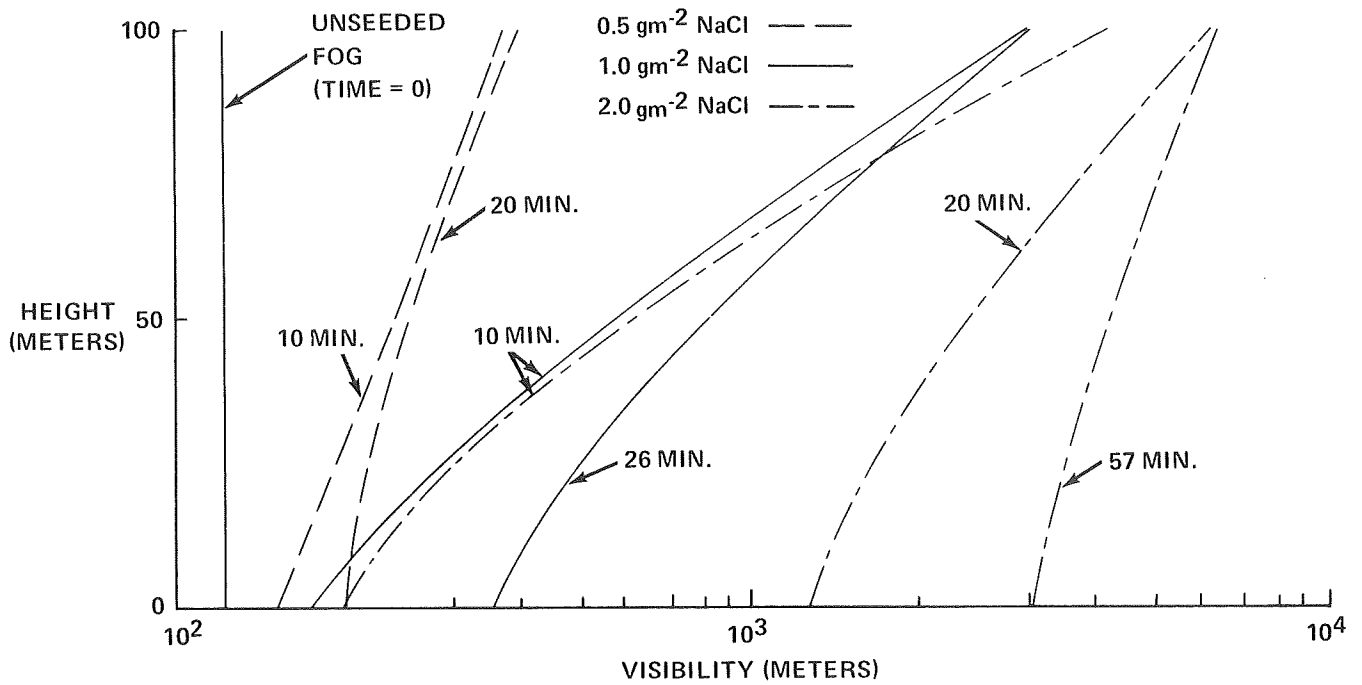


Figure 12 COMPUTED CURVES OF VISIBILITY VS. HEIGHT AS A FUNCTION OF SEEDING RATE AND TIME AFTER DEPOSITION OF NaCl SEEDING MATERIAL AT TOP OF FOG

the fog and the maximum visibility improvement was achieved (there being no mechanism for the degradation of visibility improvement in the present simulation). It is seen that the maximum visibility improvement is relatively modest, with visibility ranging from about 200 m at the ground to 400 m at the top of the fog.

With the 1.0 g m^{-2} concentration of NaCl, the visibility at the top of the fog improved to three kilometers in 10 minutes, but visibility at the ground reached only 170 m by that time. After 26 minutes, when all of the solution drops had fallen out of the fog, the visibility at the ground improved to a maximum of 360 m.

With the 2.0 g m^{-2} concentration of NaCl, which was certainly achieved over limited areas of seeded region in the actual experiment, the visibility improvement after 10 minutes was not materially better than that produced by the 1.0 g m^{-2} concentration. After 20 minutes, however, a visibility of over one kilometer was produced throughout the depth of fog. After 57 minutes, when all of the solution droplets had fallen out of the fog, the visibility reached three kilometers at the ground and $6 \frac{1}{2}$ kilometers at the top of fog.

It is important to note the increases in time required for the complete fallout of the solution drops formed on the NaCl particles with increases in the seeding rate. This is caused by greater reductions in the relative humidity, which result in the decreased growth and retarded sedimentation of the solution drops. For example, the relative humidity reductions produced by the 0.5 g m^{-2} concentration of NaCl were only a few hundredths of a percent throughout the depth of the fog. On the other hand, the 2.0 g m^{-2} concentration of NaCl reduced the relative humidity to 98% at the ground, 97% at the 50 m level, and 94% at the top of fog.

Because of this effect, it would seem desirable in this type of seeding situation to employ somewhat larger particle sizes (at the expense of requiring greater seeding rates) to obtain reasonably rapid sedimentation in the presence of sizable relative humidity reductions and thereby minimizing targeting problems. In the actual seeding experiment, it appears that this

effect may have been unintentionally achieved through partial clumping of the seeding material in dissemination.

In the above example, the computer model was used to simulate the vertical structure of the fog dissipation produced in an aerial seeding experiment based on the assumption of horizontal homogeneity. The instantaneous line source modification of the computer model, on the other hand, has been used to simulate the effects of horizontal turbulent diffusion on the vertical structure of the fog dissipation produced by a single isolated trail of seeding material dispensed by an aircraft. Because of recent recognition of the important role that turbulent diffusion may have in warm fog modification (General Discussion, NASA Symposium, 1969), the results of several simulations of the latter type will be discussed.

In each of the following examples, the seeding material is NaCl. It is assumed that the initial spread of the salt plume as a result of circulations produced by the seeding aircraft is $\sigma_y = 10 m$, corresponding to total spread of 1-1/2 to 2 times the wing span of small twin engine seeding aircraft.

The model fog is assumed to be 100 m in depth, and the effectiveness of seeding is computed at six vertical levels spaced 20 m apart. Prior to seeding, the fog is approximated by a monodisperse distribution of 20 micron diameter drops having a concentration of 62 drops cm^{-3} . It is assumed that these drops are formed on NaCl nuclei having a mass of 7.7×10^{-13} g. This monodisperse fog drop distribution produced a horizontal and a vertical visibility of 100 m, and a liquid water content of $0.26 g m^{-3}$. The model fog is based on surface measurements in fairly severe fogs at the experimental site near Elmira, New York. For simplicity, it is assumed that these conditions apply throughout the depth of the fog, thereby neglecting any variations in the properties of the natural fog with height. The fog temperature is assumed to be $10^{\circ}C$.

Figure 13 shows the computed changes in vertical visibility as a function of time after aerial seeding of the fog top with various amounts of 20 micron diameter NaCl particles. The computed vertical visibilities correspond

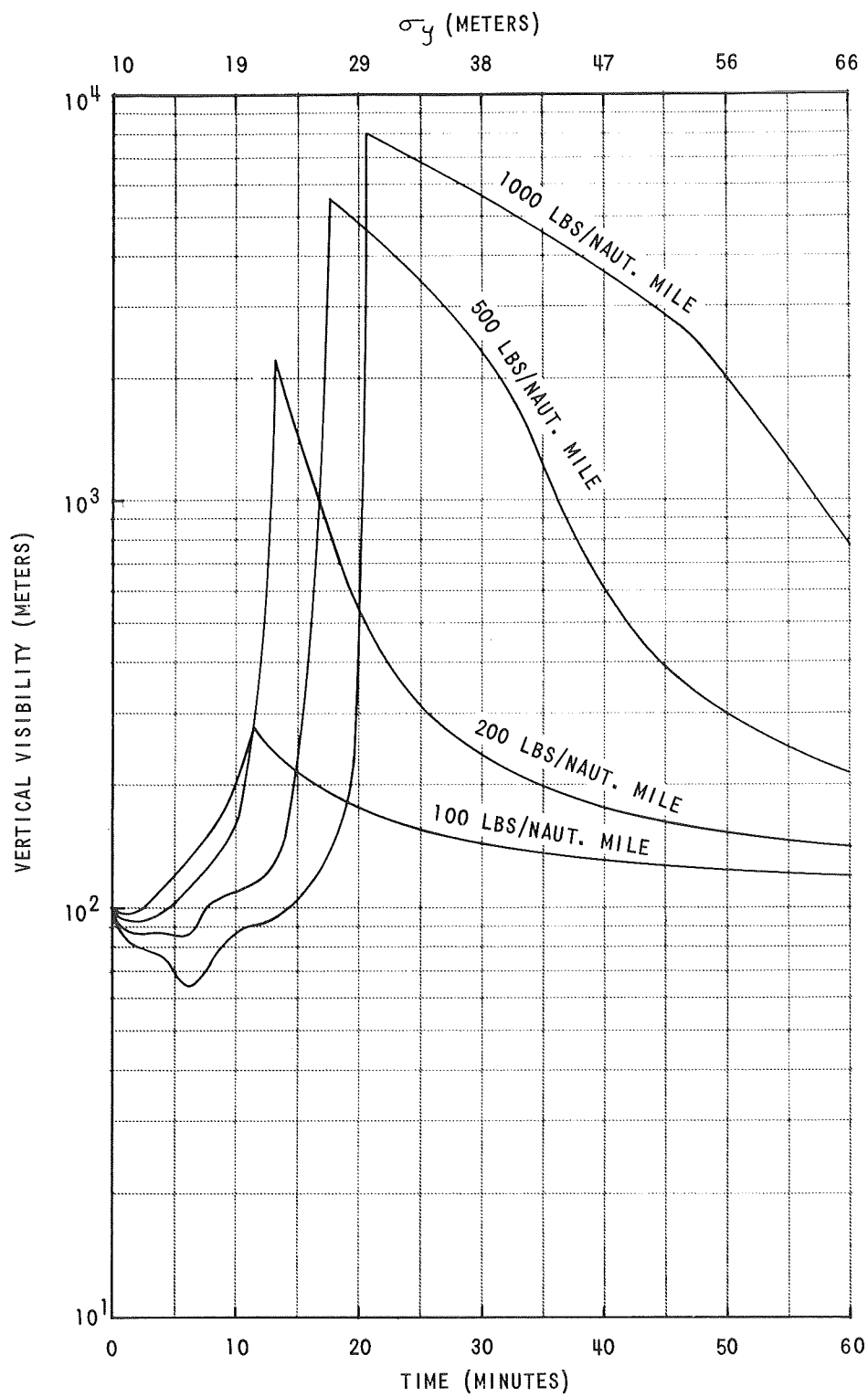


Figure 13 COMPUTED CURVES OF VERTICAL VISIBILITY VS. TIME AS A FUNCTION OF SEEDING RATE FOR AERIAL SEEDING WITH 20μ DIAMETER NaCl PARTICLES UNDER NEAR-NEUTRAL STABILITY AND A ONE KNOT WIND

to the slant range visibilities through the fog. Based upon the Smith and Hay (1961) description [Eq. (18)], the turbulent diffusion assumed in the simulations corresponds to near-neutral conditions ($i = 0.1$) with a one-knot wind or stable conditions ($i = 0.05$) with a four-knot wind.

The peak values in the vertical visibility curves in Figure 13 are reached when the solution drops completely fall out of the fog. Reformation of the fog in the modified region under the influence of horizontal turbulent diffusion is the sole mechanism in the simulations for the degradation in the visibility improvement which occurs after the fall-out of the solution drops.

Although the maximum visibility improvement in the case of the 200 lbs per nautical mile seeding rate is quite high, it will be noted that the rapid reformation of the fog, even under these low wind conditions, causes this seeding rate to be of marginal effectiveness. By employing higher seeding rates, greater and longer-lasting visibility improvements can be produced, although it is seen from Figure 13 that the time required for the maximum visibility improvement to be reached increases as the seeding rate increases, thereby increasing targeting problems. This results from the greater reductions in relative humidity that are produced by higher seeding rates, and accompanying reduced growth and slower fall-out of the solution drops.

At high rates of aerial seeding on the fog top, the solution drops remove so much water vapor from the atmosphere (in addition to causing the almost complete evaporation of the natural fog drops) that the liquid water content embodied in the pulse of solution drops as they fall through the fog can become many times the liquid water content of the natural fog. This can produce a period of horizontal visibility degradation accompanying the solution drops as they fall through the fog. In Figure 13, this is manifest in the reduced vertical visibilities shown in the first few minutes after seeding*, where the region of almost complete fog dissipation above the pulse of falling solution droplets is not yet of sufficient vertical extent to overcome the effects of

*The small ripples in the computed curves in the first few minutes after seeding result from the calculation of the effects of seeding at a limited number of vertical levels in the model fog.

the visibility degradation in the pulse of solution drops. It is seen that this effect is accentuated with increased seeding rate.

Vertical turbulent diffusion, which is neglected in the present computer model, can be important in supplementing sedimentation in transporting the solution drops down into the lower regions of the fog. In addition, vertical diffusion will act to distribute the large relative humidity reductions produced near the top of fog more uniformly throughout the depth of the fog. Both these effects will tend to increase the fog modification effectiveness of a given aerial seeding rate and reduce the time required to produce significant visibility improvement.

For the level of turbulent diffusion represented in Figure 13, however, vertical diffusion data given by Turner (1969) indicates that the standard deviation of the vertical spread σ_z will be less than 10 m after 20 minutes and at most of order 20 m after an hour. Since the 20 m spacing of the vertical levels in the model fog implies a vertical averaging of the effects of seeding over an effective σ_z of 10 m, the neglect of vertical diffusion in the computer model is not likely to produce any significant errors in the computed values of the vertical visibilities before the fall-out of the solution drops. Thereafter, the vertical gradients in the fog properties tend to decrease with increasing time so that it is still a reasonable approximation to neglect the effects of vertical diffusion in computing the vertical visibility curves shown in Figure 13.

It should be remembered that the visibility improvements shown in Figure 13 are computed for the centerline of the modified region. While the details of the cross-line distribution of modification have yet to be investigated, the standard deviations σ_y shown at the top of Figure 13 should constitute an approximate measure of the half-width of the effective region of modification. The expanding of the region of modification, as represented by an increase in σ_y with time, is an important effect of turbulence. It allows the modification of a relatively large area of a fog by making a moderate number of parallel aerial seeding passes. In the present example, a spacing between parallel seeding passes on the order of 50 to 60 m should provide fairly

uniform and long-lasting fog modification with seeding rates in excess 200 lbs per nautical mile.

In Figure 14, the visibility improvements produced by a 500 lb per nautical mile seeding rate are shown for several sizes of NaCl particles. The turbulence characteristics are as in the previous example. The results illustrate the trade-off between seeding payload requirements and speed of clearing that dictates an optimum range of hygroscopic particle sizes (Kocmond and Jiusto, 1968) for a particular seeding situation. In this case, NaCl particles between 20 and 30 μ in diameter would appear to be the best compromise. If it is deemed desirable to minimize targeting problems by employing somewhat larger particles, the payload requirements for comparable clearing become considerably greater.

The results obtained with a realistic size distribution of seeding material are shown in Figure 15. In this case, a commercially available* 15 to 40 μ diameter size distribution of NaCl particles with mean volume diameter of 29 μ was approximated in the model by nine size classes. The turbulence conditions are as above. The rounding of peaks in the vertical visibility curves and the somewhat reduced peak effectiveness compared with the idealized monodisperse distributions of NaCl are both characteristic of even the best sized commercially available hygroscopic seeding materials. In many cases, the seeding rates required to produce good fog modification with commercially available size distributions of hygroscopic seeding materials have been computed to be approximately twice the seeding rates required with idealized monodisperse distributions with the same mean diameter.

It should be noted, however, that there is no degradation of the vertical visibility in the first few minutes after seeding as was seen with the monodisperse NaCl distributions. The finite size range NaCl particles in the present case produces solution drops with a range of fall velocities which greatly spreads out the effective pulse of solution drops and eliminates the initial vertical visibility degradation.

*Meteorology Research, Inc., Altadena, California

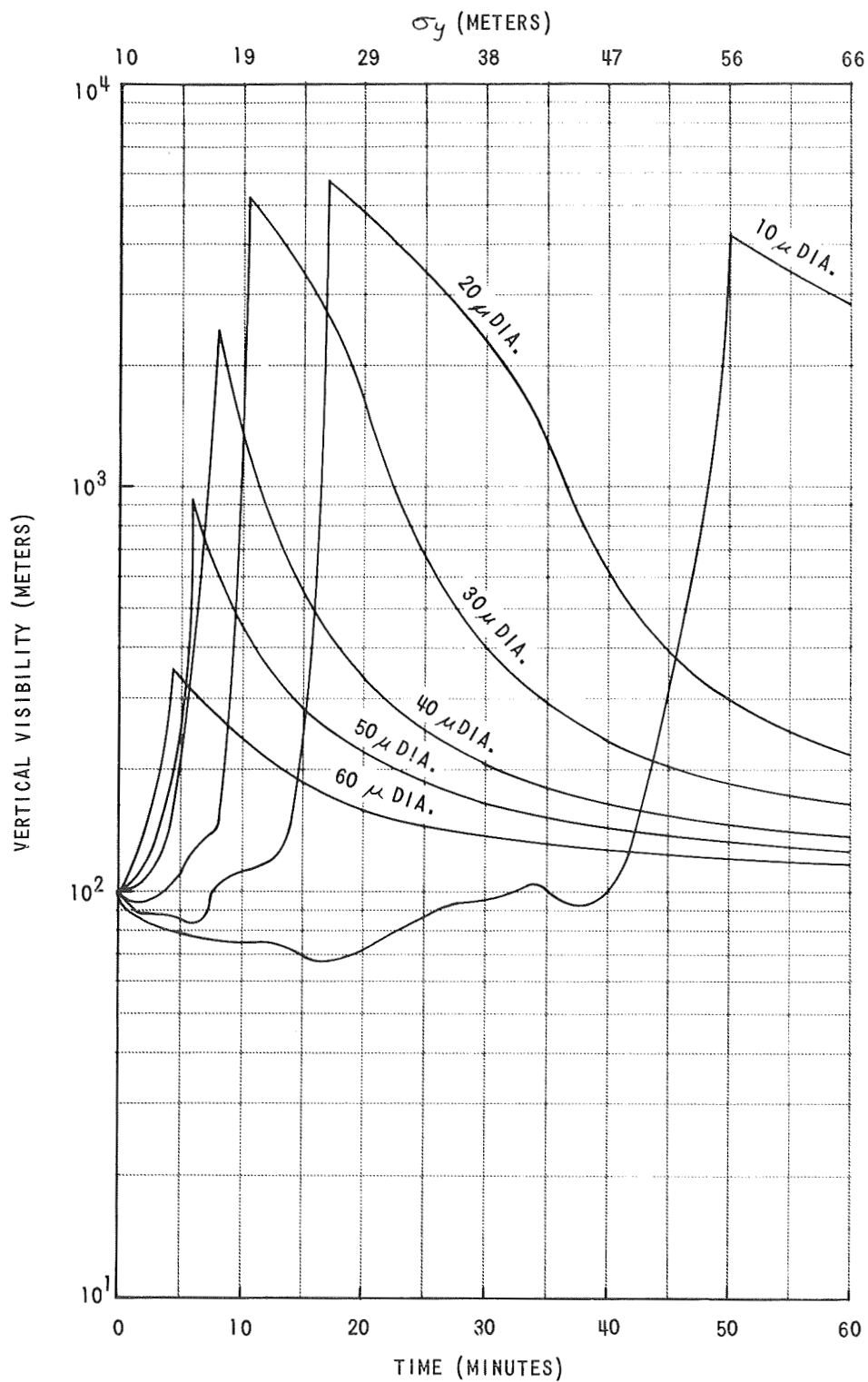


Figure 14 COMPUTED CURVES OF VERTICAL VISIBILITY VS. TIME AS A FUNCTION OF PARTICLE DIAMETER FOR AERIAL SEEDING WITH 500 LBS OF NaCl PER NAUTICAL MILE UNDER NEAR-NEUTRAL STABILITY AND A ONE KNOT WIND

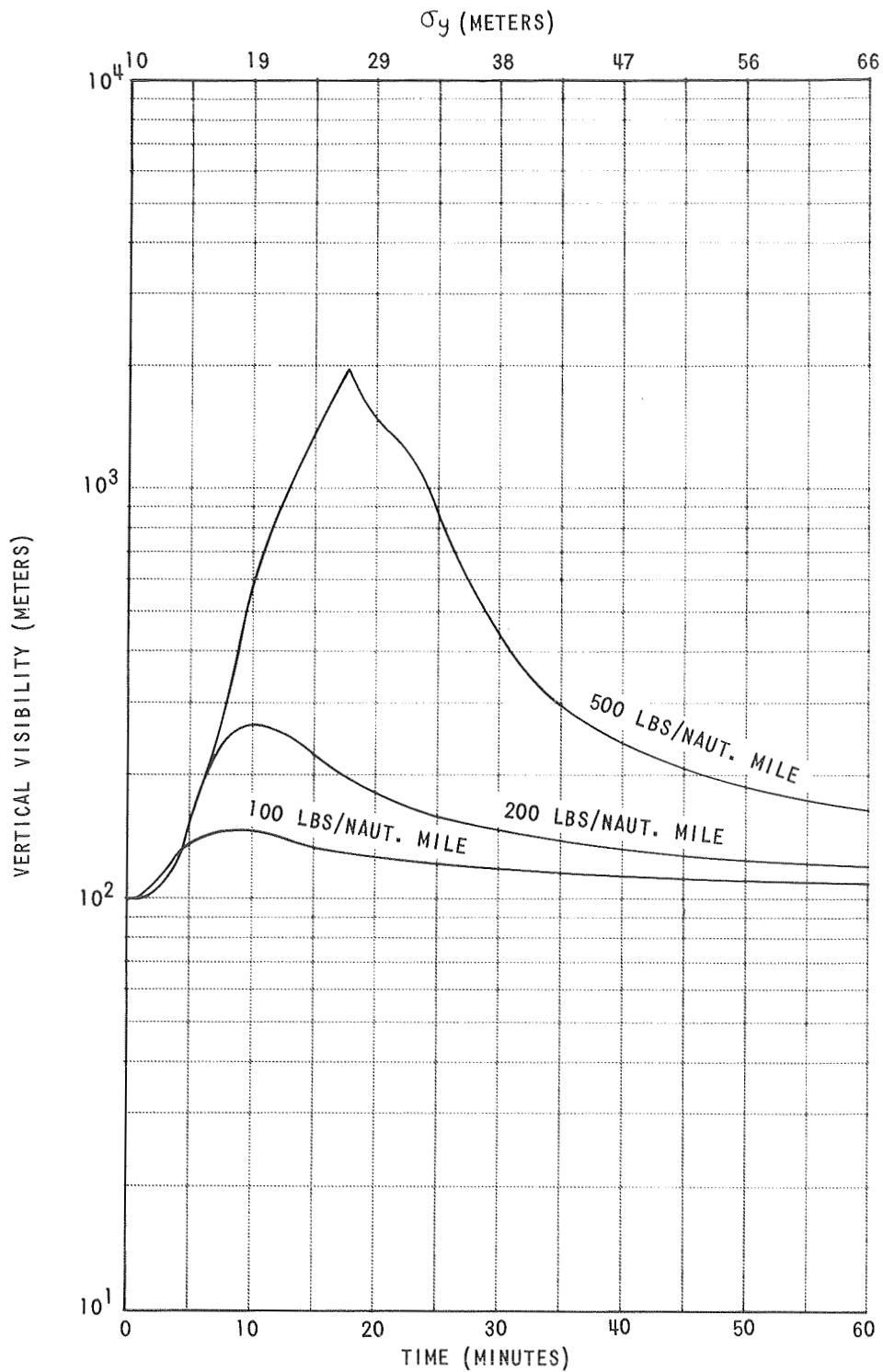


Figure 15 COMPUTED CURVES OF VERTICAL VISIBILITY VS. TIME AS A FUNCTION OF SEEDING RATE FOR AERIAL SEEDING WITH A 15 TO 40 μ DIAMETER SIZE DISTRIBUTION OF NaCl PARTICLES UNDER NEAR-NEUTRAL STABILITY AND A ONE KNOT WIND

Analysis of wind and temperature data gathered in valley fogs during the field experimentation program indicates that conditions after fog formation are much less stable than formerly thought and may approach neutral stability. To delineate the seeding rates that are required to produce significant clearing under near-neutral conditions and moderate winds, the effects of aerial seeding with 20μ diameter NaCl particles were investigated for near neutral stability ($i = 0.1$) and a five-knot wind. The results are shown in Figure 16. It is seen that parallel aerial seeding passes spaced on the order of 100 to 150 m apart with seeding rates in excess of 500 lbs per mile may be required to produce effective fog modification in this case.

With the greater turbulent diffusion, however, the neglected effects of vertical diffusion may result in significantly better visibility improvement than is shown in Figure 16. In addition, the effects of horizontal diffusion may be somewhat overestimated by employing the approximate relation of Smith and Hay (1961) [Eq. (18)] , instead of their more general expression for σ_y which takes the influence of scale of turbulent into account. Nevertheless, the above results serve to indicate that the modification of warm fogs by seeding with modest amounts (see earlier analytic estimates by Kocmond and Jiusto, 1968) of sized hygroscopic nuclei will require careful planning and execution in situations with more intense turbulent diffusion.

Based upon the simulations with the computer model discussed above, it is seen that, within the framework of the simplifying assumptions employed, the computer model provides a powerful and versatile tool for the planning and analysis of fog modification experiments. If the modification concept is to become a widespread operational reality, it should be evident that computer modeling has an important role to play in the optimization of seeding techniques for a wide variety of warm fog situations.

It is planned that future work in the area of computer modeling will be devoted to delineating the details of the influences of horizontal turbulence on the distribution of fog modification across a modified region in cases of single and multiple pass aerial seeding. It is also considered important to incorporate the effects of vertical diffusion and coalescence into the computer

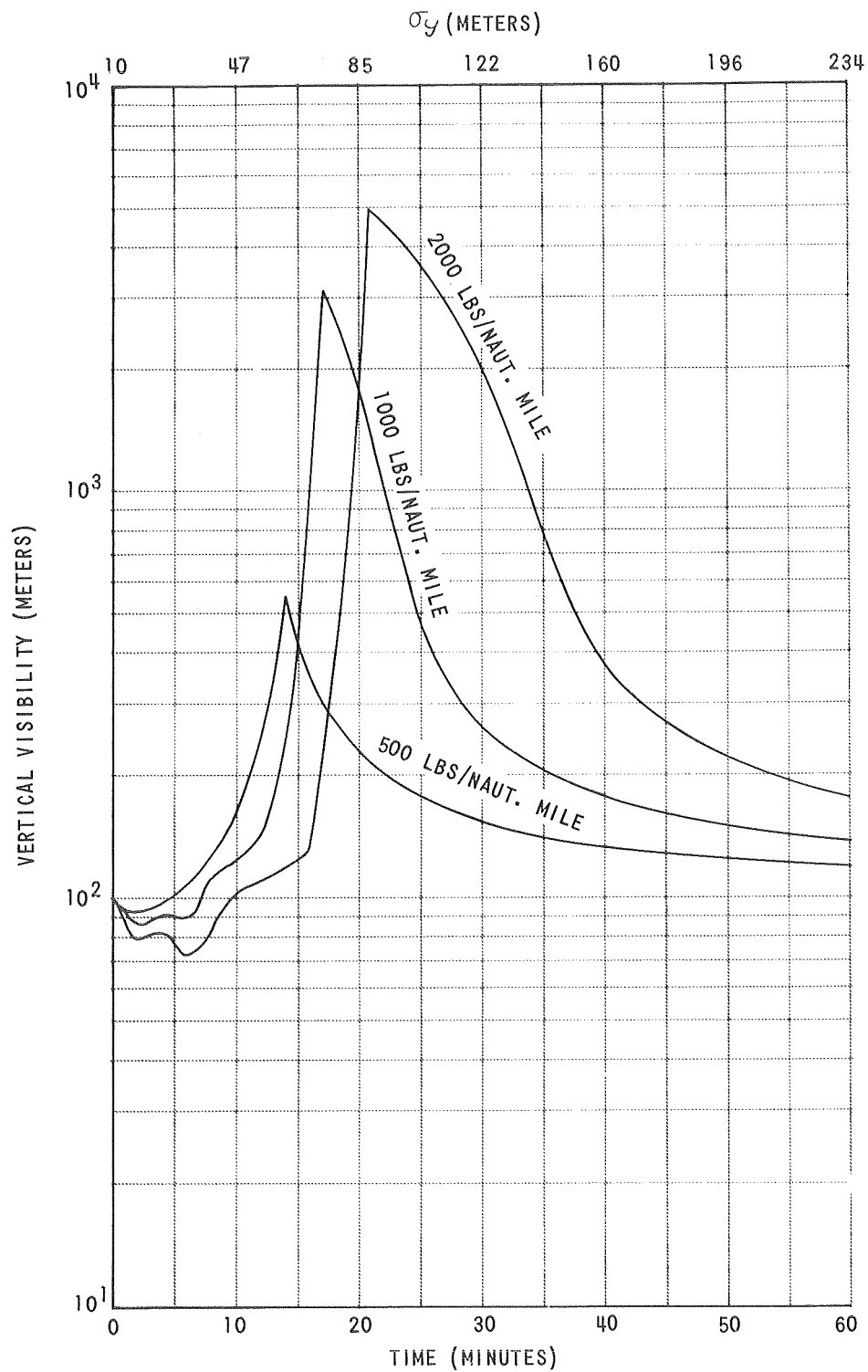


Figure 16 COMPUTED CURVES OF VERTICAL VISIBILITY VS. TIME AS A FUNCTION OF SEEDING RATE FOR AERIAL SEEDING WITH 20 μ DIAMETER NaCl PARTICLES UNDER NEAR-NEUTRAL STABILITY AND A FIVE KNOT WIND

model. With the addition of vertical diffusion, the computer model should provide an important theoretical framework for the investigation of fog formation processes as well.

IV. LABORATORY EXPERIMENTS WITH SEEDING AGENTS OTHER THAN NaCl

One of the objectives of this year's research has been to investigate the potential of various seeding agents other than NaCl for use in fog dissipation studies. From the onset of our research we have recognized that high strength aluminum alloys, as well as other metals, are susceptible to stress-corrosion cracking when repeatedly exposed to certain kinds of saline solutions.

In spite of this drawback, NaCl was initially chosen for laboratory and field evaluation because of its high efficiency in promoting droplet growth and its ease of handling. As a natural sequence to the field experiments we have turned our attention to studies of non-corrosive chemicals that might be used in place of salt. Some of the recent laboratory evaluations of chemicals look promising. Other tests, including evaluations of a wide variety of polyelectrolytes, have shown that certain chemicals have very little effect on fog.

A. Test Procedure

Fogs were produced in the 600 m³ cloud chamber shown in Figure 17. The facility consists of a cylindrical chamber which can be pressurized or evacuated at controlled rates. Consequently, nearly adiabatic expansions can be produced and under appropriate initial humidity conditions, fogs form. These laboratory fogs were found to possess physical characteristics (i.e., liquid water content, drop-size distributions, drop concentration and visibility) that are representative of natural fogs. By varying the processes of fog formation and persistence in the chamber, conditions typical of either radiation or advection fogs could be produced.

In a typical experiment, the procedure used to evaluate the seeding agent was to produce one fog for use as a control and observe its characteristics as a function of time. A second fog was then produced in an identical manner and seeded with a predetermined amount of the selected material. In both the control and seeded fogs a slow secondary expansion was initiated to cause the fogs to persist.

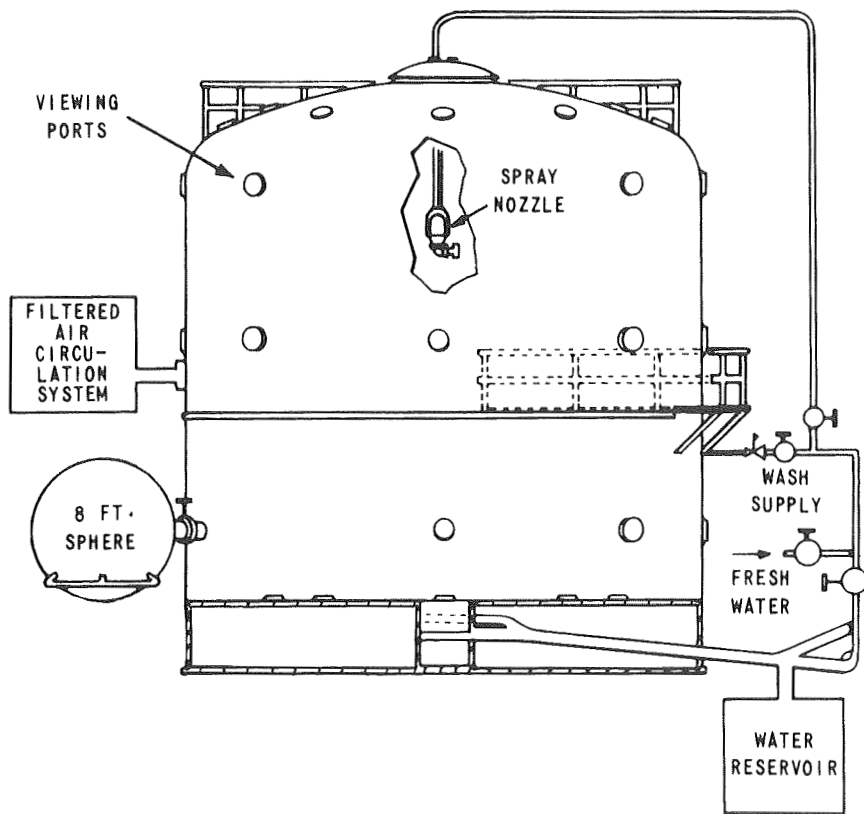


Figure 17 THE 600m³ TEST CHAMBER AT ASHFORD, NEW YORK

Seeding nuclei were dispersed into the fog from the chamber top and allowed to settle through the fog volume. When solutions were tested, droplets were injected into the fog by a droplet disseminator located approximately 25 feet above the chamber floor.

For a more detailed discussion of the fog generation process and experimental procedures, see NASA SP-212.

B. Summary of Results

The primary objective of this series of laboratory tests was to determine the maximum visibility improvement that could be achieved by seeding with various non-corrosive seeding agents and to compare these results with data obtained from seeding experiments using NaCl particles of carefully controlled size. A secondary objective was to provide further verification of our previous conclusions regarding the importance of careful control of the size distribution of seeding agents.

Table II summarizes the maximum visibility improvements obtained in 18 experiments performed with hygroscopic seeding agents that appear to have some promise. Additional seeding experiments in which polyelectrolytic chemicals were used as seeding agents will be discussed in more detail later.

The data in Table II suggest that NaCl, urea, and certain phosphates are effective in promoting laboratory fog dissipation. Careful sizing of the disodium phosphate (95% of the particles were between 4 and 20 μ) was, in part, responsible for the high efficiency of that material. A 9:1 mixture of $\text{NH}_4\text{NO}_3 \cdot \text{urea} \cdot \text{water}$ (4 parts NH_4NO_3 , 3 parts urea, and 0.78 parts distilled water) was also tested and found to be effective; however, differences in seeding procedure (liquid dissemination vs. dry particle seeding) make direct comparisons with the dry seeding agents less meaningful. Improved methods of droplet dissemination and sizing would undoubtedly result in further visibility increases when seeding with the prepared 9:1 solution.

Table II
 VISIBILITY IMPROVEMENT FACTORS* FOR SOME SEEDING
 AGENTS TESTED IN THE 600m³ CLOUD CHAMBER

SEEDING MASS	SEEDING AGENT	PARTICLE DISTRIBUTION		MAX. VISIBILITY IMPROVEMENT FACTOR
		MODE (μ)	SIZE RANGE (μ)	
5 gm	NaCl	4	90% 1-9	7.5
5 gm	NaCl	8	85% 1-11	6.2
5 gm	NaCl		95% 5-20	24.0
10 gm	NaCl	8	85% 1-11	13.2
125 gm	NaCl		44-125	6.1
5 gm	UREA		4-20	6.6
6 gm	NH ₄ NO ₃ UREA WATER	4	2-20	1.5
15 gm	NH ₄ NO ₃ UREA WATER	4	2-20	4.7
30 gm	NH ₄ NO ₃ UREA WATER	4	2-20	6.1
5 gm	CALCIUM CHLORIDE			5.8
5 gm	SODIUM NITRATE		5-40	2.0
5 gm	DISODIUM PHOSPHATE		95% 4-20	7.1
5 gm	MONOSODIUM PHOSPHATE		68% 4-20	4.8
5 gm	HEXAPHOSPHATE		58% 4-20	2.7
5 gm	SODIUM BICARBONATE			3.1
5 gm	DIAMMONIUM PHOSPHATE		62% 4-20	3.7 to 8.4
5 gm	TETRAPOTASIUM PHOSPHATE		61% 4-20	4.8
5 gm	POLYSACCHARIDE		10-20	1.9
5 gm	CABOT RESIN		10-20	1.7

* VISIBILITY IMPROVEMENT FACTOR IS DEFINED AS THE RATIO OF THE VISIBILITY OF THE SEEDED FOG TO THE VISIBILITY OF THE CONTROL FOG AT THE SAME TIME AFTER INITIATION OF THE EXPANSION

In Figure 18 the effects of seeding laboratory fog with 5 gm of disodium phosphate (Na_2HPO_4) are shown. The curves typify the manner in which visibility improvements occur after seeding laboratory fogs. In this example visibility improved by a factor of seven within 10 minutes after seeding.

Drop-size distributions obtained in this experiment about 15 minutes after seeding are compared in Figure 19 with data taken in the control fog at the same time after the start of the fog forming expansion. Note the substantial shift in drop sizes and change in drop concentration in the seeded fog. At the time these samples were taken, the liquid water content in the seeded fog had already been depleted by sedimentation and fall-out of the largest drops formed on the seeding nuclei. Prior to seeding the characteristics of the two fogs were the same in all significant respects.

From previous laboratory fog seeding experiments, it has been found that two processes are responsible for producing the visibility improvements after seeding. Initially, improvement in visibility results from a favorable shift in the drop-size distribution from one consisting of a large concentration of small droplets to one containing fewer, but larger drops. Accompanying the change in drop sizes is a decrease in the amount of scattered light (extinction coefficient) and hence an increase in visibility even though the liquid water content of the fog is somewhat increased. As time progresses, precipitation of droplets causes a decrease in the liquid water content of the fog and further improvement in visibility.

The size distribution of material used for seeding experiments is of particular importance and must be given careful attention when considering field application of the hygroscopic seeding technique. A number of experiments were performed in the laboratory to determine the effects of particle size distribution on fog dissipation efficiency. The results of one series of tests using NaCl nuclei of differing sizes are shown in Table III. Note that as the percentage of particles in the desired size range ($\sim 5\mu$ to 20μ diameter) increases the maximum visibility improvement factor also increases.

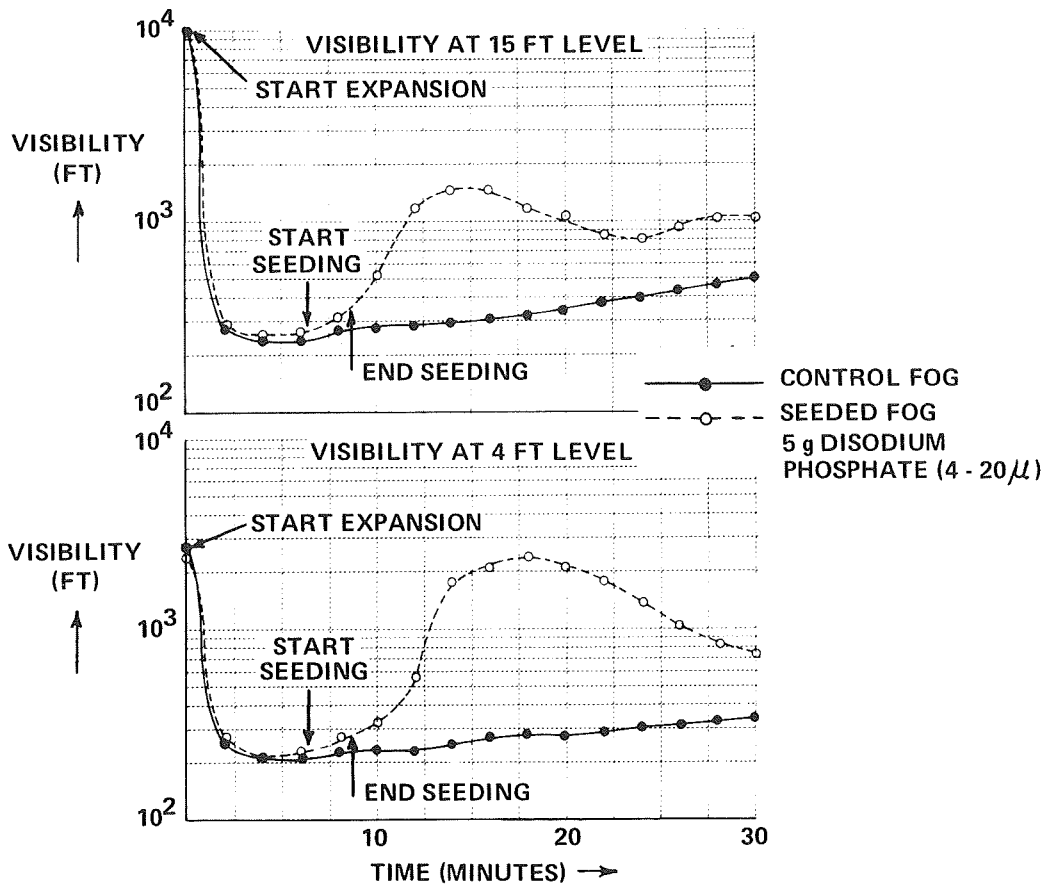


Figure 18 VISIBILITY AS A FUNCTION OF TIME FOR A SEEDED AND CONTROL FOG

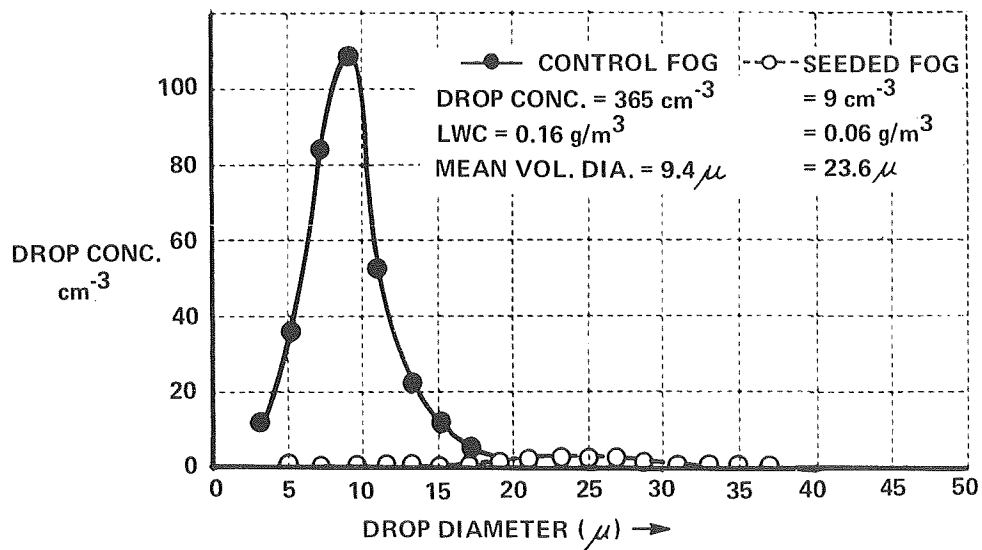


Figure 19 DROP SIZE DISTRIBUTION FOR A CONTROL FOG AND A SEEDED FOG AT T = 20 MIN. Na_2HPO_4

Table III
EFFECTS OF PARTICLE SIZE DISTRIBUTION FOR NaCl SEEDINGS
IN THE 600m³ CLOUD CHAMBER (5.0gm PAYLOADS)

PARTICLE SIZE DIAMETER	MAXIMUM VISIBILITY IMPROVEMENT FACTOR
MRI 5-20 ~ 95% 5 TO 20 μ	24.0
MORTON 200 ~ 70% 2 TO 30 μ	10.7
1 μ \leq 90% \leq 9 μ (4 μ MODE)	6.9
1 μ \leq 85% \leq 11 μ (8 μ MODE)	6.2
LESLIE MICRO POWDER (50% < 1 μ)	3.2

The results are in agreement with theory and demonstrate that carefully sized hygroscopic materials are considerably more effective in producing fog dissipation. Similar tests with other materials (i. e., urea and disodium phosphate) produced results that were compatible with these data.

Because of the increased attention given to polyelectrolytes as fog modification agents by commercial weather modification firms, a number of experiments were performed in the laboratory to determine the influence of these chemicals on visibility in fog. The results of several laboratory seeding experiments in which sized polyelectrolytes were used are summarized in Table IV. In Appendix A, chemical information about each of the chemicals tested is presented. Both cationic and anionic chemicals were

Table IV
POLYELECTROLYTE SEEDING EXPERIMENTS

SEEDING AGENT	SEEDING MASS	PARTICLE SIZE (μ)	MAXIMUM VISIBILITY IMPROVEMENT FACTOR
NALCO LN-767-193A	5.0 gm	10-20	1.8
NALCO LN-767-193B	5.0 gm	20-44	1.5
NALCO LN-767-193D	5.0 gm	20-44	1.7
NALCO LN-767-193C	75.0 gm		NONE
DOW POLY B	5.0 gm	20-44	1.3
DOW POLY B	15.0 gm	20-44	1.3
DOW SEPARAN AP 30	5.0 gm	20-44	1.2
GANEX V-904	15.0 gm	44-125	1.5
PEI-1000			NONE
RETEN 210	5.0 gm	10-20	1.5
HERCULES CMC-12MB	5.0 gm	10-20	2.3
HERCULES EHEC-755	5.0 gm	10-20	NONE
HERCULES RETEN A-1	5.0 gm	10-20	NONE

tested. As shown, the polyelectrolytes did not significantly alter visibility after seeding, in spite of the fact that care was taken to carefully size the materials and to insure adequate residence times of the particles in the fog. Differences in the amount of seeding material did not influence the results. Not apparent from the data, but nonetheless an important factor when considering the use of polyelectrolytes for field experiments, is the fact that each of the chemicals tested produced an extremely slippery surface on the chamber floor after seeding--a condition which probably could not be tolerated for airport applications.

As with experiments in which hygroscopic seeding materials were used, pertinent data on fog characteristics were collected throughout the tests involving polyelectrolytes. The data were analyzed to determine whether or not polyelectrolytes were producing physical changes in the fog that could eventually lead to visibility improvements. The results, which were consistent for all materials tested, are illustrated below.

Figure 20 shows representative visibility curves for a laboratory fog seeded with a sized polyelectrolyte--in this case, a type of polyacrylamide. Obviously, there is very little difference between the control and seeded fogs. Drop samples were collected at five-minute intervals throughout this experiment and hence drop-size distributions were determined. From the visibility data and drop size distribution data, droplet concentration and liquid water content were estimated. The results of the analysis of one drop-size distribution, obtained at the time of maximum visibility improvement (factor of 1.3) are shown in Figure 21. The results of this analysis, which show that the polyelectrolytes produced virtually no change in the physical characteristic of the fog, are typical of the results of all experiments in which such seeding agents were used.

Note also that in both the control and seeded fogs the liquid water content (LWC), drop concentration and mean volume diameter of the droplets are nearly alike. The small differences that can be detected are within the accuracy of our measuring techniques. In all our tests to date there has been no evidence of any physical mechanism attributable to polyelectrolytes that could produce the desired fog clearing.

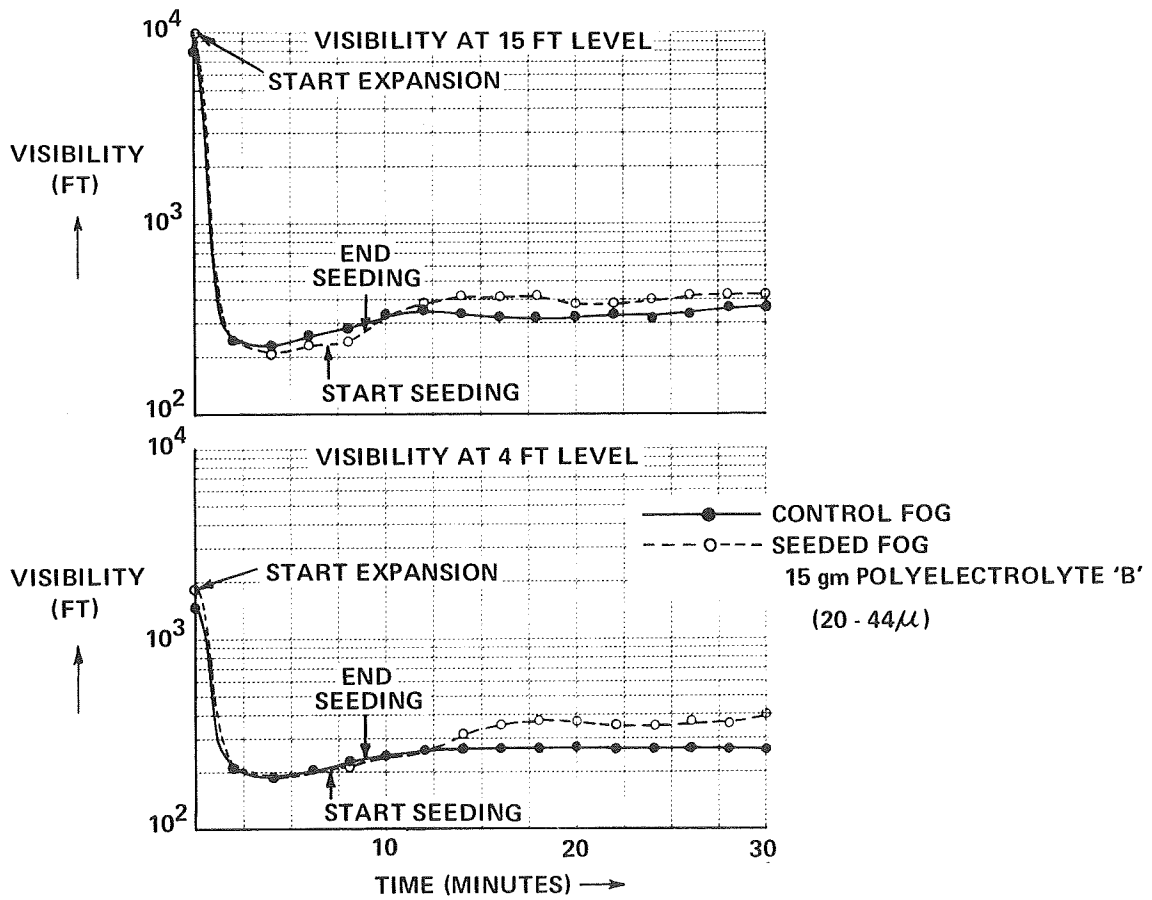


Figure 20 VISIBILITY AS A FUNCTION OF TIME FOR A SEEDED AND CONTROL FOG

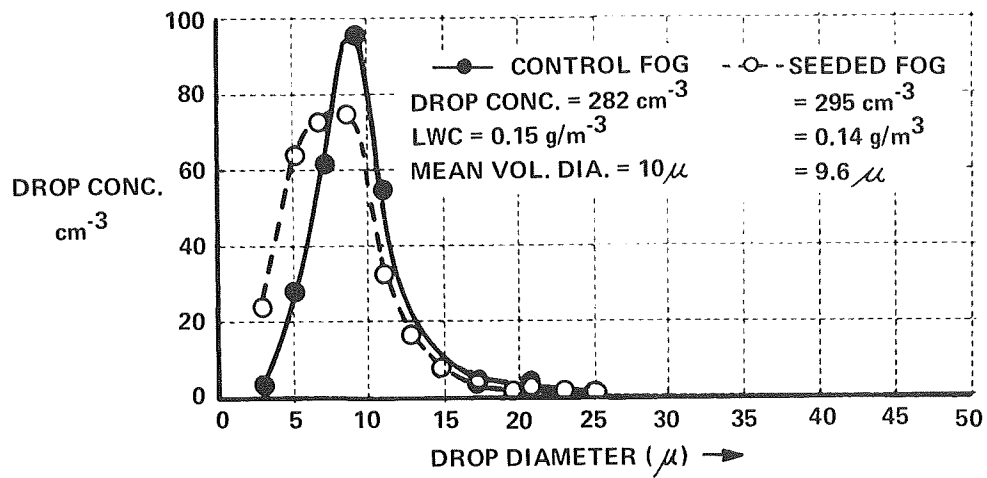


Figure 21 DROP SIZE DISTRIBUTION FOR A CONTROL FOG AND A SEEDED FOG AT T = 25 MIN. POLYELECTROLYTE 'B'

C. Conclusions

Tests performed in the laboratory have shown that a variety of hygroscopic materials other than NaCl are effective fog modifying agents. A wide cross section of polyelectrolytes were also evaluated and found to be ineffective as seeding agents.

Of the less corrosive materials tested, urea and disodium phosphate appear most promising. Additional tests are planned to determine the corrosive effects (stress corrosion cracking) of these materials on high strength aluminum alloys and to establish the gross effects that these seeding agents have on vegetation. Field testing of the materials will be performed during the fall of 1969.

REFERENCES

- Aroesty, J., and L.R. Koenig, 1969: Note on the Temperature and Evaporation of Small Drops. J. Atmos. Sci., 26, 780-782.
- Best, A.C., 1950: Empirical formulae for the terminal velocity of water drops falling through the atmosphere. Quart. J. Roy. Meteor. Soc., 76, 302-311.
- Cramer, H.E., G.M. DeSanto, R.K. Dumbauld, P. Morgenstern, and R.N. Swanson, 1964: Meteorological prediction techniques and data systems. GCA Technical Report No. 64-3-G, Geophysics Corporation of America, Bedford, Mass.
- Fletcher, N.H., 1962: The Physics of Rainclouds, Cambridge University Press.
- Jiusto, J.E., 1964: Investigation of Warm Fog Properties and Fog Modification Concepts, NASA Contractor Report CR-72.
- Jiusto, J.E., R.J. Pilié, and W.C. Kocmond, 1968: Fog Modification with Giant Hygroscopic Nuclei. J. Appl. Meteor., 7, 860-869.
- Kocmond, W.C., and J.E. Jiusto, 1968: Investigation of Warm Fog Properties and Fog Modification Concepts, NASA Contractor Report CR-1071.
- Low, R.D.H., 1969: A Generalized Equation for the Solution Effect in Droplet Growth. J. Atmos. Sci., 26, 608-611.
- Lumley, J.L., and H.A. Panofsky, 1964: The Structure of Atmospheric Turbulence. Interscience Pub., New York.
- Middleton, W.E.K., 1952: Vision Through the Atmosphere, University of Toronto Press.
- Mordy, W.A., 1959: Computations of the growth by condensation of a population of cloud droplets. Tellus, 11, 16-44.
- NASA Symposium, 1969: Progress of NASA Research on Warm Fog Properties and Modification Concepts. NASA SP-212.
- Pilié, R.J., W.C. Kocmond, and J.E. Jiusto, 1967: Warm Fog Suppression in Large-Scale Laboratory Experiments. Science, 157, 1319-1320.
- Smith, F.B. and P.F. Abbott, 1961: Statistics of lateral gustiness at 16 m above ground. Quart. J. Roy. Meteor. Soc., 87, 549-561.

_____, and J.S. Hay, 1961: The expansion of clusters of particles in the atmosphere. Quart. J. Roy. Meteor. Soc., 87, 82-101.

Squires, P., 1952: The growth of cloud drops by condensation. I. General characteristics. Aust. J. Sci. Res. A, 5, 59.

Turner, D.B., 1969: Workbook of Atmospheric Dispersion Estimates. Public Health Service Publication No. 999-AP-26.

APPENDIX A

Chemical information supplied by the manufacturer of each seeding agent tested:

<u>Trade Name</u>	<u>Chemical Nature</u>
1. NALCO LN-767-193A	High molecular weight non-ionic acrylamide
2. NALCO LN-767-193B	Anionic polymer - sodium salt of polyacrylamide
3. NALCO LN-767-193D	Anionic polymer - sodium salt of carboxylic acid
4. NALCO LN-767-193C	Cationic polymer - quarternary amine
5. Dow Polyelectrolyte 'B'	Cross-linked polyacrylamide - potassium polyacrylate copolymer
6. Dow Separan AP 30	80% polyacrylamide - sodium polyacrylate copolymer
7. PEI 1120	High m.w. polymer formed from the polymerization of ethylenimine
8. Hercules RETEN A-1	Anionic polyelectrolyte (polyacrylamide)
9. Hercules Reten 210	Cationic polyelectrolyte (no other information supplied by Hercules)
10. Hercules CMC-12M8	Sodium carboxymethyl cellulose
11. Hercules EHEC-75S	Ethyl hydroxyethyl cellulose
12. GANEX V-904	Polyvinylpyrrolidone